General Bending of Beams | 10

The theory of homogeneous bending of non-symmetric elastic beams with constant cross-section forms a central part of the mechanics of structures. The theory combines the possibility of general cross-section properties with the simultaneous bending about two axes, and thus constitutes a natural extension of the simple plane bending treated in Chapters 3–4 and developed into simple finite elements for analysis of plane frames in Chapter 7. The general theory of beam bending has wide application, e.g. to beams in buildings, bridge decks in concrete, steel or composites, or in a very general form to wind turbine blades with changing aerodynamic closed cross-section.

The basic problem is illustrated by the cantilever shown in Fig. 10.1. The load consists of a force $\mathbf{P} = [P_x, P_y, P_z]^T$ applied to the tip of the cantilever. The components are given with respect to a $\{x, y, z\}$ coordinate system with axial coordinate x and cross-section coordinates y and z as shown in the figure. The load introduces tension N and bending moments $M_y(x)$ and $M_z(x)$ in the beam, and this leads to extension and curvature. If the beam cross-section is symmetric with respect to the y and the z-axis and the force is applied to the intersection of the axes of symmetry, the problem is immediately resolved

S. Krenk, J. Høgsberg, *Statics and Mechanics of Structures*,
DOI 10.1007/978-94-007-6113-1_10,

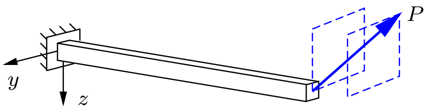

Fig. 10.1: Bending of cantilever.

into the three independent problems consisting of extension and bending in the xy and xz-planes as illustrated in Fig. 10.2. It will be demonstrated that this decomposition into extension and two plane bending problems can be obtained for a homogeneous elastic beam of general cross-section, when the axial force is applied to the *elastic center*, and the two planes of bending are determined as the *principal axes* of the cross-section. The theory is developed for beams with non-homogeneous distribution of elastic stiffness over the cross-section.

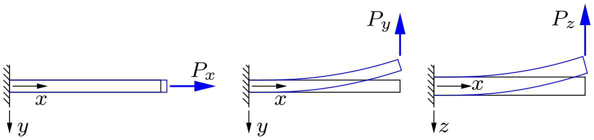

Fig. 10.2: Extension and bending of cantilever beam.

The bending of an elastic beam of constant but general cross-section is treated in Section 10.1. When bending a beam with symmetric cross-section in its plane of symmetry, the strain is proportional to the distance from the neutral axis. This concept is generalized by considering the strain distribution to be a linear function of both the cross-section coordinates. The result is a systematic theory of bending, originally developed by Navier (1785–1836). The theory relates the normal force N and the two bending moment components M_y and M_z at a cross-section to the corresponding set of kinematic quantities: the axial strain ε_0, and the two curvature components κ_y and κ_z. The constitutive relations that relate the section force components N, M_y, M_z to their kinematic counterparts $\varepsilon_0, \kappa_y, \kappa_z$ depend on the cross-section geometry and the distribution of elastic stiffness over the cross-section. These properties are contained in a set of cross-section parameters like area, moment of inertia etc. and Section 10.2 describes how the cross-section parameters are obtained from the geometry and stiffness distribution in the cross-section. This analysis identifies the *elastic center* where a normal force will only produce extension, and a set of *principal axes* that uncouples the two bending problems. Even if not using these axes directly the fact that bending can be uncoupled if choosing these axes constitutes an important characteristic of beam bending, that is essential for the understanding of the associated mechanisms. The bending parameters relating to different axes are connected by a transformation that is quite similar to that of the plane stress component transformation dealt with in Section 8.4. As a consequence the Mohr circle construction also illustrates the relation of bending stiffness around different axes, and concept of principal axes associated with minimum and maximum bending stiffness. As discussed in Section 10.3, the linear distribution of the axial strain over the cross-section in general bending leads to a simple explicit relation for the distribution of the axial stress component. The axial stress constitutes an important design parameter. The axial stress distribution also serves as a step in the determination of the shear stress distribution associated with non-homogeneous bending as discussed in Chapter 11.

10.1 Bending of non-symmetric beams

The theory of bending of beams with non-symmetric cross-section is based on a simple extension of the corresponding theory for plane bending. The basic assumption is that the beam is homogeneous and loaded by a combination of a normal force and two bending moment components, that are constant over the beam. This constitutes a logical generalization of the concept of homogeneous bending and permits the development of a fairly simple and rigorous theory of bending of homogeneous beams. Like in the case of plane bending, the idea is to develop the deformation characteristics from the ideal case of homogeneous bending, and then to assume its validity also in cases with moment variation along the beam. The procedure is to first define the kinematics and then to derive the associated stresses and section forces.

10.1.1 Kinematic formulation

When a beam is in a state of homogeneous bending and extension, symmetry suggests that plane cross-sections remain plane under the deformation. This implies that a cross-section that originally coincides with the yz-plane will have an axial displacement $u(y, z)$ in the form of a linear function of y and z as illustrated in Fig. 10.3. The mathematical form is

$$u(y, z) = u_0 + y\,\eta_y + z\,\eta_z\,, \tag{10.1}$$

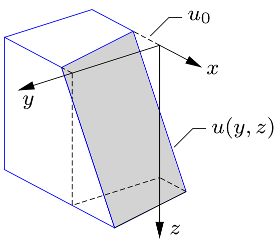

Fig. 10.3: Linear distribution of axial displacement $u(y, z)$.

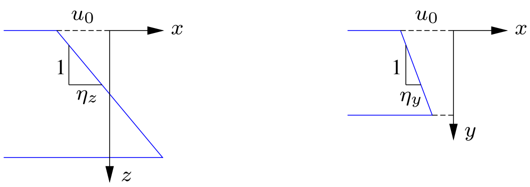

Fig. 10.4: Linear variation of axial displacement in coordinate planes.

where $u_0 = u(0,0)$ is the axial displacement of the origin of the coordinate system. Furthermore, it is found by differentiation that η_y and η_z are the inclinations of the cross-section in the y- and z-direction, respectively. The variation of the axial deformation along the cross-section axes y and z is illustrated in Fig. 10.4, where u_0 is shown as the axial displacement at the origin of the coordinate system, and η_y and η_z are the inclinations of the axes after deformation. Within a 'small deformation' theory a similar representation applies to the other cross-sections, and thus the axial displacement u_0 as well as the inclinations η_y and η_z are functions of the axial coordinate x,

$$u_0 = u_0(x)\,, \qquad \eta_y = \eta_y(x)\,, \qquad \eta_z = \eta_z(x)\,. \tag{10.2}$$

However, to keep the notation as compact as possible, the argument x is implied and not written explicitly in the following derivations.

The axial strain is the derivative of the axial displacement $u(x,y,z)$ with respect to the longitudinal coordinate x,

$$\varepsilon(y,z) \;=\; \frac{\partial u}{\partial x} \;=\; \varepsilon_0 \,+\, y\,\kappa_y \,+\, z\,\kappa_z\,, \tag{10.3}$$

where ε_0 is the axial strain at the origin, and κ_y and κ_z are defined by the inclinations,

$$\varepsilon_0 \;=\; \frac{du_0}{dx}\,, \qquad \kappa_y \;=\; \frac{d\eta_y}{dx}\,, \qquad \kappa_z \;=\; \frac{d\eta_z}{dx}\,. \tag{10.4}$$

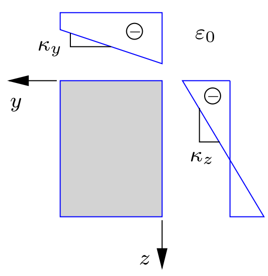

Fig. 10.5: Plot of linear strain variations along the y and z axes.

It follows from (10.3) that the distribution of the axial strain is linear over the cross-section, conveniently illustrated by the linear variation of the strain along the y- and z-axes, as shown in Fig. 10.5. The strain at the origin of the yz-coordinate system is ε_0, and the gradient of the normal strain is given by the components κ_y and κ_z.

The section inclinations η_y and η_z – and thereby the parameters κ_y and κ_z – are related to the transverse displacement of the beam. In the present case of pure bending there is no twist of the beam, and thus the transverse displacement is a translation, described by the motion of a single point, e.g. the origin of the yz-coordinate system,

$$v(x,y,z) \;=\; v_0(x)\,, \qquad w(x,y,z) \;=\; w_0(x)\,. \tag{10.5}$$

The two shear strain components associated with the x-component can now be calculated based on the displacement representations (10.1) and (10.5),

$$\gamma_{xy} \;=\; \frac{dv_0}{dx} + \eta_y\,, \qquad \gamma_{xz} \;=\; \frac{dw_0}{dx} + \eta_z\,. \tag{10.6}$$

These relations define the x-derivative of the transverse displacements as

$$\frac{dv_0}{dx} \;=\; -\eta_y + \gamma_{xy}\,, \qquad \frac{dw_0}{dx} \;=\; -\eta_z + \gamma_{xz}\,. \tag{10.7}$$

These relations are the general form of the plane bending relation (4.29) of Timoshenko beam theory.

The shear strains defined via (10.6) are constant over any cross-section, and thus represent only an average value. A more detailed analysis of the *shear stress* distribution over the cross-section is typically obtained directly from a static analysis as discussed in Chapter 11. As demonstrated in Section 4.3 the contribution from the shear strains to the beam displacements is often negligible, and this contribution is therefore often neglected in the kinematics of the beam. The result is the Bernoulli beam theory, in which the inclinations are given by

$$\eta_y \;=\; -\frac{dv_0}{dx}\,, \qquad \eta_z \;=\; -\frac{dw_0}{dx}\,. \tag{10.8}$$

The parameters κ_y and κ_z are then given as the curvatures of the beam axis by the relations

$$\kappa_y \;=\; -\frac{d^2v_0}{dx^2}\,, \qquad \kappa_z \;=\; -\frac{d^2w_0}{dx^2}\,. \tag{10.9}$$

These relations generalize the kinematic relations (4.17) and (4.18) of plane bending.

10.1.2 Stresses and section forces

In Bernoulli beam theory it is assumed that the deformation is not constrained in the transverse direction. The axial stress is then obtained directly from the axial strain (10.3) by multiplication with the elastic modulus E. This gives the expression

$$\sigma(y,z) \;=\; E\,\varepsilon(y,z) \;=\; E\,\big(\varepsilon_0 + y\,\kappa_y + z\,\kappa_z\big), \tag{10.10}$$

where the elastic modulus $E = E(y,z)$ may vary over the cross-section. While the strain distribution (10.3) is linear in the coordinates y and z a non-homogeneous elastic stifness may lead to a more complicated stress variation.

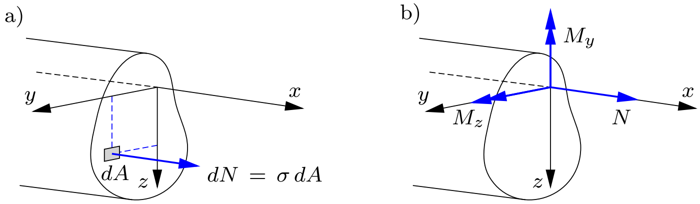

Fig. 10.6: Contribution of a) normal stress in dA to b) section forces.

The three section forces associated with the homogeneous beam bending problem are the normal force N and the two bending moments M_y and M_z with respect to axes of the cross-section coordinate system. Figure 10.6 shows an arbitrary cross-section with normal stress distribution σ given by the expression (10.10). Now, consider an infinitesimal part of the cross-section with area dA. As indicated in Fig. 10.6a the contribution to the normal force from this infinitesimal area is

$$dN \;=\; \sigma(y,z)\,dA\,. \tag{10.11}$$

The normal force component dN also introduces bending moments with respect to the reference coordinate system. In the present context it is convenient to introduce moment components such that M_y is formed via the moment arm y and M_z is formed via the moment arm z, and thus

$$dM_y \;=\; \sigma\,y\,dA\,, \qquad dM_z \;=\; \sigma\,z\,dA\,. \tag{10.12}$$

The corresponding moment vector components are shown in Fig. 10.6b. The resulting section forces are obtained by integration over the cross-section area,

$$N \;=\; \int_A \sigma\,dA\,, \quad M_y \;=\; \int_A \sigma\,y\,dA\,, \quad M_z \;=\; \int_A \sigma\,z\,dA\,. \tag{10.13}$$

By substitution of the expression for the normal stress (10.10) into (10.13a) the normal force is expressed as

$$N = \varepsilon_0 \int_A E\,dA + \kappa_y \int_A E\,y\,dA + \kappa_z \int_A E\,z\,dA \tag{10.14}$$

in terms of the reference strain ε_0 and the curvature components κ_y and κ_z. Similar expressions for the bending moments can be found by substitution of (10.10) into (10.13b,c), whereby

$$\begin{aligned} M_y &= \varepsilon_0 \int_A Ey\,dA + \kappa_y \int_A Ey^2\,dA + \kappa_z \int_A Ezy\,dA\,, \\ M_z &= \varepsilon_0 \int_A Ez\,dA + \kappa_y \int_A Eyz\,dA + \kappa_z \int_A Ez^2\,dA\,. \end{aligned} \tag{10.15}$$

The area integrals are cross-section parameters representative of axial, bending and coupling stiffness with respect to the yz-axes.

The integrals contain the elastic modulus E, that may depend on the location in the cross-section. To keep full generality E is therefore kept inside the integral. The beam stiffness parameters combine the elastic stiffness and the geometry of the cross-section and in order to keep this format a reference elastic modulus E_0 is introduced. The cross-section parameters can be expressed in matrix format as

$$E_0 \begin{bmatrix} F & S_y & S_z \\ S_y & I_{yy} & I_{yz} \\ S_z & I_{zy} & I_{zz} \end{bmatrix} = \int_A E \begin{bmatrix} 1 & y & z \\ y & y^2 & yz \\ z & zy & z^2 \end{bmatrix} dA\,. \tag{10.16}$$

Note, that the matrix is symmetric, thereby containing six cross-section parameters.

For homogeneous elastic stiffness with $E = E_0$ the notation implies that the cross-section parameters $F, S_y, \cdots$ represent geometric characteristics of the cross-section like area, static moment etc. In the general format F is defined by the weighted area integral

$$F = \frac{1}{E_0} \int_A E\,dA\,. \tag{10.17}$$

For a homogeneous cross-section with constant elastic modulus $E = E_0$ the weighted area F recovers the geometric area A, defined by

$$A = \int_A dA\,. \tag{10.18}$$

The parameters S_y and S_z are the weighted static moments,

$$S_y = \frac{1}{E_0}\int_A E\,y\,dA\,, \qquad S_z = \frac{1}{E_0}\int_A E\,z\,dA\,. \tag{10.19}$$

Finally, I_{yy}, I_{zz} and $I_{yz} = I_{zy}$ are the weighted moments of inertia,

$$I_{yy} = \frac{1}{E_0}\int_A E\,y^2\,dA\,, \quad I_{zz} = \frac{1}{E_0}\int_A E\,z^2\,dA\,, \quad I_{yz} = \frac{1}{E_0}\int_A E\,yz\,dA\,. \tag{10.20}$$

It is often convenient to choose E_0 as the elastic modulus of the dominant material in the cross-section. For instance, in the case of reinforced concrete beams E_0 is typically chosen as the elastic modulus of the concrete, whereby $E/E_0 = 1$ for the concrete part of the cross-section, while E/E_0 is approximately 15 for the small areas representing the steel reinforcement. This is illustrated in Example 10.3.

When introducing the cross-section parameters defined in (10.16) into the expressions (10.14) and (10.15) for the section forces, these can be combined into matrix form as

$$\begin{bmatrix} N \\ M_y \\ M_z \end{bmatrix} = E_0 \begin{bmatrix} F & S_y & S_z \\ S_y & I_{yy} & I_{yz} \\ S_z & I_{zy} & I_{zz} \end{bmatrix} \begin{bmatrix} \varepsilon_0 \\ \kappa_y \\ \kappa_z \end{bmatrix}. \tag{10.21}$$

This matrix relation represents the general constitutive relation between the section forces N, M_y and M_z and the associated generalized deformation measures ε_0, κ_y and κ_z. The normal force in (10.14) can be written directly as

$$N = E_0\big(F\varepsilon_0 + S_y\kappa_y + S_z\kappa_z\big)\,, \tag{10.22}$$

while the bending moments are

$$\begin{aligned} M_y &= E_0\big(S_y\varepsilon_0 + I_{yy}\kappa_y + I_{yz}\kappa_z\big)\,, \\ M_z &= E_0\big(S_z\varepsilon_0 + I_{yz}\kappa_y + I_{zz}\kappa_z\big)\,. \end{aligned} \tag{10.23}$$

It is observed that for an arbitrarily located cross-section coordinate system all three deformation parameters ε_0, κ_y and κ_z contribute to each of the section forces N, M_y and M_z. However, a special coordinate system may be determined in which there are three independent deformation mechanisms – extension and two curvatures – each corresponding to a single section force – the normal force and bending moments about two suitably defined axes. This corresponds to the diagonal form of the matrix relation (10.21). The determination of this so-called *principal coordinate system* is an important part of the cross-section analysis, treated next.

10.2 Cross-section analysis

In general, diagonalization of the bending stiffness matrix in (10.21) consists of a translation of the cross-section coordinate system to the so-called *elastic center*, followed by a rotation. The translation leads to uncoupling of the normal force relation from the bending relations. Sometimes it is convenient to use the intermediate coordinate system through the elastic center, in which the normal force relation is uncoupled from the moment relations, while the coupled form of the two-component bending problem is retained.

10.2.1 Elastic center

Initially, the coupling between extension and bending is eliminated by a suitable translation of the coordinate system to a reference point $[c_y, c_z]$, as illustrated in Fig. 10.7. Hereby, new cross-section coordinates $\{\bar{y}, \bar{z}\}$ are introduced via

$$y = \bar{y} + c_y\,, \qquad z = \bar{z} + c_z\,. \tag{10.24}$$

Substitution of these relations into the kinematic expression for the axial displacement in (10.1) gives the axial displacement with respect to the new translated coordinate system,

$$u(\bar{y}, \bar{z}) = u_0 + (\bar{y} + c_y)\eta_y + (\bar{z} + c_z)\,\eta_z = u_c + \bar{y}\,\eta_y + \bar{z}\,\eta_z\,. \tag{10.25}$$

In this expression u_c is the axial displacement at the origin of the translated coordinate system,

$$u_c = u_0 + \eta_y c_y + \eta_z c_z\,. \tag{10.26}$$

It is seen from (10.25) that the inclinations in the new coordinate system are still η_y and η_z. Thus, a translation of the coordinate system, as shown in Fig. 10.7, has no influence on the cross-section inclinations.

The corresponding axial strain is obtained by differentiation of the axial displacement in (10.25) with respect to the longitudinal coordinate x,

$$\varepsilon(\bar{y}, \bar{z}) = \varepsilon_c + \bar{y}\,\kappa_y + \bar{z}\,\kappa_z\,, \tag{10.27}$$

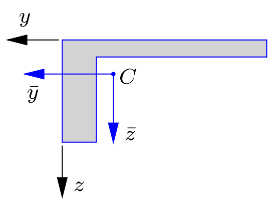

Fig. 10.7: Coordinate system centered at C.

where $\varepsilon_c = \partial u_c/\partial x$ is the axial strain at the reference point $[c_y, c_z]$, while $\kappa_y = \partial \eta_y/\partial x$ and $\kappa_z = \partial \eta_z/\partial x$ are the same curvatures as in the original coordinate system, illustrated in Fig. 10.5. The axial stress is obtained by multiplication of the strain ε by the elastic modulus E,

$$\sigma(\bar{y},\bar{z}) = E\,\varepsilon(\bar{y},\bar{z}) = E\,\varepsilon_c + E\,\bar{y}\,\kappa_y + E\,\bar{z}\,\kappa_z\,. \tag{10.28}$$

The section forces in the new coordinate system are obtained by integration over the cross-section area as

$$N = \int_A \sigma\,dA\,,\quad M_{\bar{y}} = \int_A \sigma\,\bar{y}\,dA\,,\quad M_{\bar{z}} = \int_A \sigma\,\bar{z}\,dA\,. \tag{10.29}$$

The bar on the moment subscripts indicate that the moments are with respect to the translated coordinate system $\{\bar{y},\bar{z}\}$. Substitution of the axial stress σ in (10.28) into the expression for the section forces in (10.29) gives the constitutive relation with respect to the new translated coordinate system. It is of similar form as the original formulation (10.21), and can be written as

$$\begin{bmatrix} N \\ M_{\bar{y}} \\ M_{\bar{z}} \end{bmatrix} = E_0 \begin{bmatrix} F & S_{\bar{y}} & S_{\bar{y}} \\ S_{\bar{y}} & I_{\bar{y}\bar{y}} & I_{\bar{y}\bar{z}} \\ S_{\bar{z}} & I_{\bar{y}\bar{z}} & I_{\bar{z}\bar{z}} \end{bmatrix} \begin{bmatrix} \varepsilon_c \\ \kappa_y \\ \kappa_z \end{bmatrix}. \tag{10.30}$$

The cross-section parameters in the above relations are defined and determined in the same way as in (10.16)–(10.20), but now with respect to the new coordinates $\{\bar{y},\bar{z}\}$.

The location of the origin $[c_y, c_z]$ of the new coordinate system is now chosen such that axial extension creates no bending moments, or conversely that axial loading only produces axial extension and no curvature. Figure 10.8 illustrates the separation of the general linear deformation into a) pure extension and b) pure rotation about C. In the constitutive relation (10.30) the coupling parameters $S_{\bar{y}}$ and $S_{\bar{z}}$ between bending and extension are now eliminated by imposing the conditions

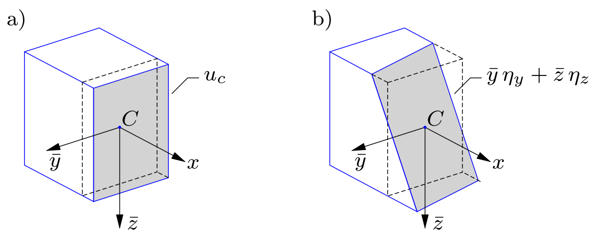

Fig. 10.8: Separation of axial displacement into a) pure extension, and b) pure bending.

$$S_{\bar{y}} = \frac{1}{E_0}\int_A E\bar{y}\,dA = \frac{1}{E_0}\int_A E(y-c_y)\,dA = S_y - c_yF = 0\,,$$
$$S_{\bar{z}} = \frac{1}{E_0}\int_A E\bar{z}\,dA = \frac{1}{E_0}\int_A E(z-c_z)\,dA = S_z - c_zF = 0\,. \tag{10.31}$$

The last equalities determine the origin $[c_y, c_z]$ of the new coordinate system as

$$c_y = \frac{S_y}{F}\,, \qquad c_z = \frac{S_z}{F}\,. \tag{10.32}$$

In the following, this point in the cross-section $[c_y, c_z]$ is referred to as the *elastic center*. For homogeneous cross-sections the elastic center coincides with the *geometric center*, while for inhomogeneous cross-sections these two centers are not equivalent. The elastic center is determined from the ratio between the weighted static moments S_y and S_z in the original reference coordinate system, and the weighted cross-section area F. Any cross-section analysis starts with the location of the elastic center, and if possible it is advantageous to choose the reference coordinate system $\{y, z\}$ to coincide with the elastic center or at least to facilitate evaluation of the integrals defining the cross-section parameters.

Static moment of a flange

Many thin-walled cross-sections are composed of rectangular parts, and the cross-section parameters are then conveniently determined by summation of the contribution from the individual rectangular parts. The basis of the procedure is be illustrated by a single rectangular flange, as shown in Fig. 10.9 together with the reference coordinate system $\{y, z\}$.

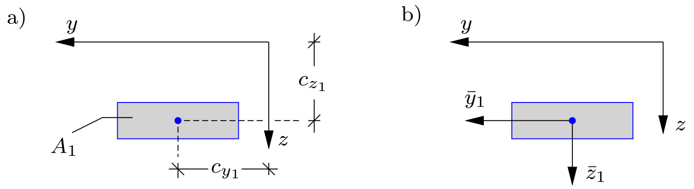

Fig. 10.9: Rectangular flange.

The weighted area of the flange is given by the area integral

$$F_1 = \frac{1}{E_0}\int_{A_1} Ey\,dA\,, \tag{10.33}$$

where the subscript 1 refers to this particular flange. For cross-sections with multiple flanges the subscripts indicate the results or parameters for the individual flanges. Assume that the position of the center of the flange is known, and given by c_{y_1} and c_{z_1} with respect to the reference coordinate system $\{y, z\}$. A change of coordinate system is introduced as in (10.24),

$$y = \bar{y}_1 + c_{y_1}, \qquad z = \bar{z}_1 + c_{z_1}, \tag{10.34}$$

where the local coordinate system $\{\bar{y}_1, \bar{z}_1\}$ for flange 1 is shown in Fig. 10.9b. The static moments S_y and S_z are defined in (10.19), and substitution of the coordinte representation (10.34) then gives

$$\begin{aligned} S_y &= \frac{1}{E_0}\int_{A_1} Ey\,dA = \frac{1}{E_0}\int_{A_1} E(\bar{y}_1 + c_{y_1})\,dA = S_{\bar{y}_1} + F_1 c_{y_1}, \\ S_z &= \frac{1}{E_0}\int_{A_1} Ez\,dA = \frac{1}{E_0}\int_{A_1} E(\bar{z}_1 + c_{z_1})\,dA = S_{\bar{z}_1} + F_1 c_{z_1}. \end{aligned} \tag{10.35}$$

When the origin of the local coordinate system $\{\bar{y}_1, \bar{z}_1\}$ is located at the center of the flange, the corresponding static moments vanish,

$$S_{\bar{y}_1} = 0, \qquad S_{\bar{z}_1} = 0. \tag{10.36}$$

Thus, the static moments of the flange with respect to the reference coordinate system $\{y, z\}$ are given by the weighted area of the flange times the distance to the center of the flange,

$$S_y = F_1\, c_{y_1}, \qquad S_z = F_1\, c_{z_1}. \tag{10.37}$$

It is important to use the correct sign of the coordinates c_{y_1} and c_{z_1} of the flange center. In Fig. 10.9 the center is located in the positive quadrant of the $\{y, z\}$ coordinate system, whereby both c_{y_1} and c_{z_1} are positive.

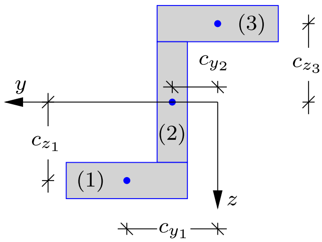

Fig. 10.10: Z-profile composed of flanges. Indication of non-zero distances to local centers.

Cross-sections are often composed of several flanges as illustrated in Fig. 10.10. The location of the elastic center of the full cross-section then depends on the resulting static moments, and thereby the sum of the contributions from the individual flanges. Based on the above result (10.37) for the single flange, the resulting static moments of a cross-section with n flanges are found by summation as

$$S_y = \sum_{j=1}^{n} F_j \, c_{y_j} \, , \quad S_z = \sum_{j=1}^{n} F_j \, c_{z_j} \, , \tag{10.38}$$

where F_j is the area weighted by the elastic modulus for flange j with center located in $[c_{y_j}, c_{z_j}]$. Thus, the determination of the static moments boils down to the determination of the weighted area and the location of the center for each individual flange.

If the elastic modulus is constant for each flange, $E(y,z) = E_j$, the expression for the static moments can be written as

$$S_y = \sum_{j=1}^{n} \frac{E_j}{E_0} A_j \, c_{y_j} \, , \quad S_z = \sum_{j=1}^{n} \frac{E_j}{E_0} A_j \, c_{z_j} \, , \tag{10.39}$$

where A_j is the geometric area and $[c_{y_j}, c_{z_j}]$ the geometric center of flange j.

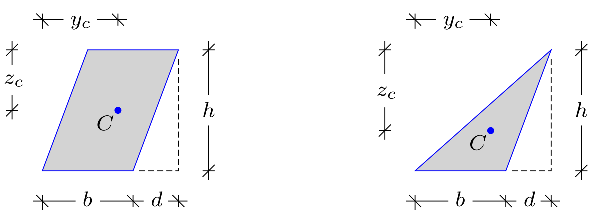

$$A = bh \qquad A = \tfrac{1}{2} bh$$
$$y_c = \tfrac{1}{2}(b+d) \qquad y_c = \tfrac{1}{3}(2b+d)$$
$$z_c = \tfrac{1}{2} h \qquad z_c = \tfrac{2}{3} h$$

Fig. 10.11: Properties of different flange geometries.

Figure 10.11 shows the geometric area and the location of the center for an skew flange and a triangle. The calculation of static moments and the location of the elastic center is illustrated in the following by examples.

Example 10.1. Elastic center for angle profile. Figure 10.12 shows a cross-section with two flanges connected at a right angle. The origin of the coordinate system $\{y, z\}$ is placed where the flanges join, and such that the axes coincide with the respective centerlines of the flanges. Hereby, there is no contribution to the static moment S_z from the horizontal flange (1), while S_y contains no contribution from the vertical flange (2). The length, thickness and elastic modulus of the horizontal flange are a_1, t_1 and E_1, and similarly with subscript 2 for the vertical flange. The elastic modulus of the horizontal flange is chosen as the reference value, i.e. $E_0 = E_1$. The cross-section is assumed to be thin-walled with $t_1 \ll a_1$ and $t_2 \ll a_2$.

The effective area of the cross-section is defined in (10.17), and with $E_0 = E_1$

$$F = \sum_{j=1}^{2} \frac{E_j}{E_1} A_j = a_1 t_1 + a_2 t_2 \frac{E_2}{E_1} \, .$$

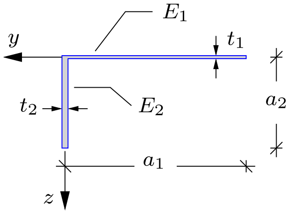

Fig. 10.12: Inhomogeneous thin-walled angle profile.

Note, that because the cross-section parameters are normalized with respect to the elastic modulus of the horizontal flange, the second term contains a scaling by the ratio of the elastic moduli. Following (10.39) the static moments are also determined by summation over the flanges. In the y-direction this gives

$$S_y = \sum_{j=1}^{2} \frac{E_j}{E_1} A_j c_{y_j} = a_1 t_1 (-\tfrac{1}{2} a_1) = -\tfrac{1}{2} a_1^2 t_1 ,$$

where the contribution from the vertical flange vanishes because the coordinate system is located such that $c_{y_2} = 0$. The center of the horizontal flange (1) is located in the negative y-direction, giving a negative value of c_{y_1} and S_y. The static moment in the z-direction is obtained in the same way as

$$S_z = \sum_{j=1}^{2} \frac{E_j}{E_1} A_j c_{z_j} = \frac{E_2}{E_1} a_2 t_2 \tfrac{1}{2} a_2 = \tfrac{1}{2} a_2^2 t_2 \frac{E_2}{E_1} ,$$

where the contribution from the horizontal flange vanishes because $c_{z_1} = 0$.

Following (10.32) the coordinates of the elastic center are found by the ratio between the weighted static moments and the weighted cross-section area. This gives the y-component

$$c_y = \frac{S_y}{F} = \frac{-\tfrac{1}{2} a_1^2 t_1}{a_1 t_1 + a_2 t_2 \dfrac{E_2}{E_1}} = -\tfrac{1}{2} a_1 \frac{1}{1 + \dfrac{a_2 t_2 E_2}{a_1 t_1 E_1}} = \frac{-\tfrac{1}{2} a_1}{1 + \dfrac{A_2 E_2}{A_1 E_1}} ,$$

and the z-component

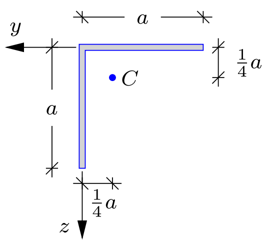

Fig. 10.13: Symmetric thin-walled angle profile.

$$c_z = \frac{S_z}{F} = \tfrac{1}{2}a_2 \frac{\dfrac{a_2t_2E_2}{a_1t_1E_1}}{1 + \dfrac{a_2t_2E_2}{a_1t_1E_1}} = \tfrac{1}{2}a_2 \frac{\dfrac{A_2E_2}{A_1E_1}}{1 + \dfrac{A_2E_2}{A_1E_1}} = \frac{\tfrac{1}{2}a_2}{\dfrac{A_1E_1}{A_2E_2} + 1} .$$

For the symmetric case with $a_1 = a_2 = a$, $t_1 = t_2$ and $E_1 = E_2$, shown in Fig. 10.13, the elastic center is located at the quarter point,

$$c_y = -\tfrac{1}{4}a , \qquad c_z = \tfrac{1}{4}a .$$

An important part of analytical cross-section analysis is the choice of reference coordinate system. Exercise 10.1 considers the location of the elastic center of the angle section in this example with respect to another reference system. □

Example 10.2. Inhomogeneous T-profile.

Figure 10.14 shows a thin-walled T-profile, where the length, thickness, elastic modulus of the flange and the web are a_f, t_f, E_f and a_w, t_w, E_w, respectively. The reference coordinate system is located such that the y- and z-axis coincide with the centerlines of the flange and web, respectively. The elastic modulus of the flange is chosen as the reference value, $E_0 = E_f$.

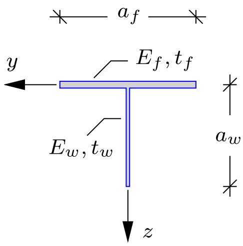

Fig. 10.14: Inhomogeneous T-profile.

The cross-section area is obtained by summation of the contributions from flange and web,

$$F = \frac{1}{E_f}\,(E_f\,a_f t_f + E_w\,a_w t_w) = a_f t_f + \frac{E_w}{E_f}\,a_w t_w = A_f + \frac{E_w}{E_f}\,A_w$$

where $A_f = a_f t_f$ and $A_w = a_w t_w$ are the geometric areas of flange and web, respectively. The static moments are determined as

$$S_y = 0 , \qquad S_z = \tfrac{1}{2}\,a_w\,A_w\,\frac{E_w}{E_f} = \tfrac{1}{2}\,a_w^2 t_w\,\frac{E_w}{E_f} .$$

Note, that $S_y = 0$ because of symmetry, and therefore it is usually advantageous to place one of the axes in the line of symmetry. The coordinates of the elastic center are

$$c_y = \frac{S_y}{F} = 0 , \quad c_z = \frac{S_z}{F} = \frac{\tfrac{1}{2}\,a_w\,A_w\,\dfrac{E_w}{E_f}}{A_f + \dfrac{E_w}{E_f}\,A_w} = \tfrac{1}{2}\,a_w \frac{\dfrac{E_wA_w}{E_fA_f}}{1 + \dfrac{E_wA_w}{E_fA_f}} = \frac{\tfrac{1}{2}\,a_w}{\dfrac{E_fA_f}{E_wA_w} + 1} .$$

A special case is $a_f = a_w = a$, $t_f = t_w$ and $E_f = E_w$, whereby $c_z = \tfrac{1}{4}\,a$.

The cross-section has a line of symmetry along the centerline of the web, and the elastic center is located on this line of symmetry. In general cross-sections with a common line of geometric and material symmetry will have the elastic center located on this line. □

Elastic center for symmetric cross-sections

For a cross-section with geometric and material double symmetry the location of the elastic center is at the intersection of the axes of symmetry, illustrated in Fig. 10.15a. However, also cross-sections formed by flanges or groups of flanges with point symmetry about a common center will have the elastic center at this point, as illustrated in Fig. 10.15b.

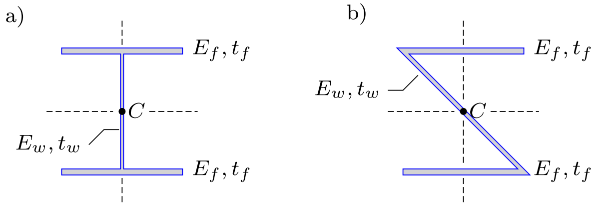

Fig. 10.15: Cross-sections with a) double symmetry, or b) point symmetry.

Example 10.3. Rectangular cross-section with reinforcement.

Figure 10.16 shows a rectangular cross-section in a concrete beam, with elastic modulus E_c and dimensions $a \times 2a$. Steel reinforcement is introduced at the bottom of the beam to improve the strength in tension. The steel reinforcement is located at vertical distance $\frac{1}{6}a$ from the bottom. The elastic modulus of steel is $E_s = 15E_c$ and the total area of the reinforcement is $A_s = \frac{1}{100}A_c = \frac{1}{50}a^2$. The cross-section is symmetric with respect to the vertical centerline. The reference coordinate system is therefore located at the top of the cross-section with the vertical z-axis coinciding with the line of symmetry. The elastic modulus of concrete is chosen as the reference value: $E_0 = E_c$.

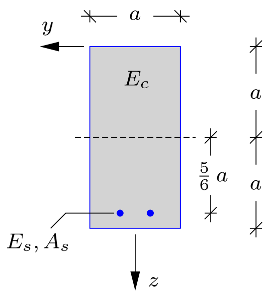

Fig. 10.16: Rectangular cross-section of concrete beam with steel reinforcement.

The weighted area is determined as the sum of the contributions from concrete and steel, and the concrete area is represented approximately by the full area of the cross-section,

$$F = \frac{1}{E_c}\left(E_c\, 2a^2 + E_s\, A_s\right) = a^2\big(2 + \tfrac{15}{50}\big) = \tfrac{23}{10}\, a^2 \,.$$

The center of the concrete part is located at vertical distance $z = a$, while the center of the steel reinforcement is located at $z = 2a - \frac{1}{6}a$. The static moment with respect to the z-axis can therefore be determined as

$$S_z = \frac{1}{E_c}\big(E_c\, 2a^2\, a + E_s\, A_s\,(2a - \tfrac{1}{6}a)\big) = \tfrac{51}{20}\, a^2 \,.$$

The elastic center is therefore located at

$$c_z = \frac{S_z}{F} = \tfrac{51}{46}\, a$$

which is slightly below the geometric center of the cross-section. □

10.2.2 Moments of inertia

By the translation of the coordinate system, whereby the origin of the coordinate system is located at the elastic center $[c_y, c_z]$, the extension and the bending problems uncouple. Hereby, the constitutive relation in (10.30) can be written as two separate relations,

$$N = E_0 F\, \varepsilon_c \,, \qquad \begin{bmatrix} M_{\bar{y}} \\ M_{\bar{z}} \end{bmatrix} = E_0 \begin{bmatrix} I_{\bar{y}\bar{y}} & I_{\bar{y}\bar{z}} \\ I_{\bar{y}\bar{z}} & I_{\bar{z}\bar{z}} \end{bmatrix} \begin{bmatrix} \kappa_y \\ \kappa_z \end{bmatrix} . \tag{10.40}$$

This leaves the determination of the moments of inertia $I_{\bar{y}\bar{y}}$, $I_{\bar{z}\bar{z}}$ and $I_{\bar{y}\bar{z}}$ with respect to the translated coordinate system. In the new coordinate system the moments of inertia are defined as

$$\begin{aligned} I_{\bar{y}\bar{y}} &= \frac{1}{E_0}\int_A E\bar{y}^2\, dA = \frac{1}{E_0}\int_A E(y - c_y)^2\, dA = I_{yy} + c_y^2 F - 2c_y S_y \,, \\ I_{\bar{z}\bar{z}} &= \frac{1}{E_0}\int_A E\bar{z}^2\, dA = \frac{1}{E_0}\int_A E(z - c_z)^2\, dA = I_{zz} + c_z^2 F - 2c_z S_z \,, \\ I_{\bar{y}\bar{z}} &= \frac{1}{E_0}\int_A E\bar{y}\bar{z}\, dA = \frac{1}{E_0}\int_A E(y - c_y)(z - c_z)\, dA \\ &\qquad\qquad\qquad\qquad\qquad = I_{yz} + c_y c_z F - c_y S_z - c_z S_y \,. \end{aligned} \tag{10.41}$$

The static moments S_y and S_z can be eliminated in terms of the coordinates of the elastic center $[c_y, c_z]$ by the relation (10.32). Hereby the expressions for the moments of inertia reduce to

$$I_{\bar{y}\bar{y}} = I_{yy} - c_y^2 F \,, \quad I_{\bar{z}\bar{z}} = I_{zz} - c_z^2 F \,, \quad I_{\bar{y}\bar{z}} = I_{yz} - c_y c_z F \,. \tag{10.42}$$

The separated format of the constitutive relations in (10.40) is quite suitable for analytical solutions, as the inverse of a 2×2 matrix has a fairly simple explicit form. This is illustrated in Section 10.3, where the axial strain and stress are determined.

Application of parallel axis theorem

The expression for the moments of inertia with respect to a translated coordinate system is often called the *parallel axis theorem*. The terms in (10.42) all involve integration over the cross-section area. As for the static moments the moments of inertia in (10.42) are determined by summation of the contribution to the moments of inertia from the individual flanges or parts of the cross-section.

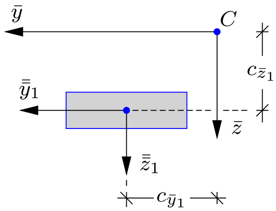

Fig. 10.17: Rectangular flange.

Figure 10.17 shows a simple rectangular flange with geometric area A_1. Assume that this flange is part of a larger cross-section, as indicated in Fig. 10.10, and that the coordinate system $\{\bar{y}, \bar{z}\}$ is located at the elastic center C of the full cross-section. A local coordinate system $\{\bar{\bar{y}}_1, \bar{\bar{z}}_1\}$ is placed at the center of the local flange in Fig. 10.17 with axes parallel to those of the $\{\bar{y}, \bar{z}\}$ coordinate system. The coordinates of the local center in the $\{\bar{y}, \bar{z}\}$ coordinate system are $c_{\bar{y}_1}$ and $c_{\bar{z}_1}$, as shown in Fig. 10.17. The relation between the two coordinate systems can be written as

$$\bar{y} = \bar{\bar{y}}_1 + c_{\bar{y}_1}, \qquad \bar{z} = \bar{\bar{z}}_1 + c_{\bar{z}_1}. \tag{10.43}$$

The contribution from the local flange to the moments of inertia with respect to the $\{\bar{y}, \bar{z}\}$ coordinate system can be determined by the integrals given in (10.41), where substitution of (10.43) gives

$$\begin{aligned}
I_{\bar{y}\bar{y}} &= \frac{1}{E_0}\int_{A_1} E(\bar{\bar{y}}_1 + c_{\bar{y}_1})^2\, dA = I_{\bar{\bar{y}}_1\bar{\bar{y}}_1} + c_{\bar{y}_1}^2 F_1, \\
I_{\bar{z}\bar{z}} &= \frac{1}{E_0}\int_{A_1} E(\bar{\bar{z}}_1 + c_{\bar{z}_1})^2\, dA = I_{\bar{\bar{z}}_1\bar{\bar{z}}_1} + c_{\bar{z}_1}^2 F_1, \\
I_{\bar{y}\bar{z}} &= \frac{1}{E_0}\int_{A_1} E(\bar{\bar{y}}_1 + c_{\bar{y}_1})(\bar{\bar{z}}_1 + c_{\bar{z}_1})\, dA = I_{\bar{\bar{y}}_1\bar{\bar{z}}_1} + c_{\bar{y}_1}c_{\bar{z}_1} F_1,
\end{aligned} \tag{10.44}$$

where it is used that in the local $\{\bar{\bar{y}}_1, \bar{\bar{z}}_1\}$ coordinate system $S_{\bar{\bar{y}}_1} = S_{\bar{\bar{z}}_1} = 0$.

For cross-sections composed of multiple flanges the summation of the contributions from each individual flange gives the resulting moments of inertia as

$$
\begin{aligned}
I_{\bar{y}\bar{y}} &= \sum_{j=1}^{n} \left(I_{\bar{\bar{y}}_j\bar{\bar{y}}_j} + c_{\bar{y}_j}^2 F_j \right) = \sum_{j=1}^{n} \left(I_{\bar{\bar{y}}_j\bar{\bar{y}}_j} + c_{\bar{y}_j}^2 A_j E_j/E_0 \right), \\
I_{\bar{z}\bar{z}} &= \sum_{j=1}^{n} \left(I_{\bar{\bar{z}}_j\bar{\bar{z}}_j} + c_{\bar{z}_j}^2 F_j \right) = \sum_{j=1}^{n} \left(I_{\bar{\bar{z}}_j\bar{\bar{z}}_j} + c_{\bar{z}_j}^2 A_j E_j/E_0 \right), \\
I_{\bar{y}\bar{z}} &= \sum_{j=1}^{n} \left(I_{\bar{\bar{y}}_j\bar{\bar{z}}_j} + c_{\bar{y}_j} c_{\bar{z}_j} F_j \right) = \sum_{j=1}^{n} \left(I_{\bar{\bar{y}}_j\bar{\bar{z}}_j} + c_{\bar{y}_j} c_{\bar{z}_j} A_j E_j/E_0 \right),
\end{aligned}
\tag{10.45}
$$

where the last equalities apply to homogeneous flanges with area A_j. This is the general form of the parallel axis theorem.

Example 10.4. Moments of inertia for rectangular cross-section. Figure 10.18 shows a homogeneous rectangular cross-section with constant elastic modulus E, width b and height h. In this case the origin of the reference coordinate system, shown in the figure, coincides with the elastic center, whereby $[\bar{y}, \bar{z}] = [y, z]$. The elastic modulus E is normalized by a reference elastic modulus E_0 to present the results in a general form.

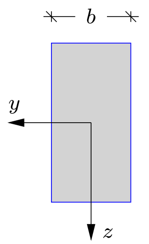

Fig. 10.18: Rectangular homogeneous cross-section.

The definition of the moments of inertia with respect to the reference axes are given by the integral in (10.16). This means that the moment of inertia in the z-direction is defined as

$$
I_{zz} = \frac{1}{E_0} \int_A E z^2 \, dA
$$

and because E is constant it can be taken outside the area integral, which can be represented by double integrals in the y- and z-coordinates,

$$
I_{zz} = \frac{E}{E_0} \int_{-\frac{b}{2}}^{\frac{b}{2}} \int_{-\frac{h}{2}}^{\frac{h}{2}} z^2 \, dz \, dy = \frac{Eb}{E_0} \int_{-\frac{h}{2}}^{\frac{h}{2}} z^2 \, dz = \frac{Eb}{E_0} \left[\tfrac{1}{3} z^3 \right]_{-\frac{h}{2}}^{\frac{h}{2}} = \tfrac{1}{12} b h^3 \, E/E_0 \, .
$$

In the case when $E = E_0$, the moment of inertia is $I_{zz} = \frac{1}{12} b h^3$. The moment of inertia with respect to the y-direction is determined similarly as

$$
I_{yy} = \tfrac{1}{12} h b^3 \, E/E_0 \, .
$$

For the coupling moment of inertia the integral separates into

$$I_{yz} = \frac{1}{E_0}\int_A Eyz\,dA = \frac{E}{E_0}\left(\int_{-\frac{b}{2}}^{\frac{b}{2}} y\,dy\right)\left(\int_{-\frac{h}{2}}^{\frac{h}{2}} z\,dz\right).$$

Because of symmetry both integrals vanish

$$\int_{-\frac{b}{2}}^{\frac{b}{2}} y\,dy = \left[\tfrac{1}{2}y^2\right]_{-\frac{b}{2}}^{\frac{b}{2}} = 0\,, \qquad \int_{-\frac{h}{2}}^{\frac{h}{2}} z\,dz = \left[\tfrac{1}{2}z^2\right]_{-\frac{h}{2}}^{\frac{h}{2}} = 0\,,$$

whereby

$$I_{yz} = 0\,.$$

Note, that only one of the integrals for I_{yz} have to vanish, and thus $I_{yz} = 0$ if at least one of the two coordinate axes is a line of symmetry. □

Example 10.5. Moments of inertia for skew cross-section. Figure 10.19 shows a skew homogeneous cross-section with elastic modulus $E = E_0$, width b and height h. The origin of the reference coordinate system in the figure coincides with the elastic center. The inclination of the cross-section is represented by the angle θ, as shown in the figure. The rectangular cross-section in Fig. 10.18 is recovered for $\theta = 0$.

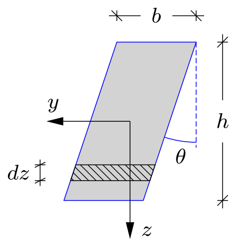

Fig. 10.19: Skew cross-section.

Consider a very thin strip of the cross-section, indicated by the hatched area in the figure. The width is b and the incremental height is dz. The coordinates of the center of the strip are $[y, z]$, with $y = z\tan\theta$. The moments of inertia for the strip are then calculated as

$$\begin{aligned} dI_{yy} &= \tfrac{1}{12}b^3\,dz + b\,dz\,y^2 = \tfrac{1}{12}b^3\,dz + bz^2\tan^2\theta\,dz\,,\\ dI_{zz} &= \tfrac{1}{12}(dz)^3 b + b\,dz\,z^2 = bz^2 dz\,,\\ dI_{yz} &= b\,dz\,zy = bz^2\tan\theta\,dz\,. \end{aligned}$$

As dz is infinitesimal, higher order terms in dz can be omitted. The moments of inertia are now obtained by integration over the height of the cross-section in the z-direction, whereby

$$I_{yy} = \tfrac{1}{12}b^3h + \tfrac{1}{12}h^3b\,\tan^2\theta\,, \quad I_{zz} = \tfrac{1}{12}h^3b\,, \quad I_{yz} = \tfrac{1}{12}h^3b\,\tan\theta\,.$$

It is seen that the results for the rectangular cross-section are recovered for $\theta = 0$. □

Example 10.6. Moments of inertia for angle profile. Figure 10.20a shows a cross-section with two thin-walled flanges connected at a right angle, similar to that in Example 10.1. In this case the cross-section is homogeneous with elastic modulus $E = E_0$. The dimensions of the horizontal and vertical flanges are $2a \times t$ and $a \times 2t$, respectively, as shown in the figure. The reference coordinate system $\{y, z\}$ is located as in Example 10.1, where the position of the elastic center was found as

$$c_y = -\tfrac{1}{2}a\,, \qquad c_z = \tfrac{1}{4}a\,.$$

The elastic center and the new coordinate system $\{\bar{y}, \bar{z}\}$ are both indicated in Fig. 10.20b.

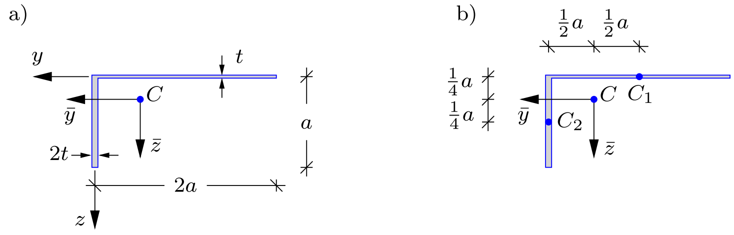

Fig. 10.20: Homogeneous thin-walled angle profile.

The centers of the two flanges are indicated in the figure as C_1 and C_2. The distance from the local center to the elastic center C is also shown in the figure. The local moments of inertia for the flanges are now determined. Both flanges are rectangular, whereby the results in Example 10.4 can be applied. For the horizontal flange 1 the local moments of inertia are:

$$I_{\bar{\bar{y}}_1\bar{\bar{y}}_1} = \tfrac{1}{12}(2a)^3 t = \tfrac{2}{3}a^3 t\,, \quad I_{\bar{\bar{z}}_1\bar{\bar{z}}_1} = \tfrac{1}{12}t^3 a \simeq 0\,, \quad I_{\bar{\bar{y}}_1\bar{\bar{z}}_1} = 0\,.$$

Since the flanges are thin-walled ($t \ll a$) any terms with higher powers of thickness are omitted because these contributions are insignificant. This is the reason for setting $I_{\bar{\bar{z}}_1\bar{\bar{z}}_1} = 0$, while the coupling moment of inertia $I_{\bar{\bar{y}}_1\bar{\bar{z}}_1}$ vanishes due to symmetry. The local moments of inertia for the vertical flange 2 are obtained similarly,

$$I_{\bar{\bar{y}}_2\bar{\bar{y}}_2} = \tfrac{1}{12}(2t)^3 a \simeq 0\,, \quad I_{\bar{\bar{z}}_2\bar{\bar{z}}_2} = \tfrac{1}{12}(a)^3 2t = \tfrac{1}{6}a^3 t\,, \quad I_{\bar{\bar{y}}_2\bar{\bar{z}}_2} = 0\,.$$

The resulting moments of inertia are found by a transformation via the parallel axis theorem to the actual coordinate system $\{\bar{y}, \bar{z}\}$, followed by summation of the contributions from the two flanges. By using (10.45) for homogeneous flanges,

$$I_{\bar{y}\bar{y}} = \left(\tfrac{2}{3}\,a^3\,t + 2at(\tfrac{1}{2}a)^2\right) + \left(0 + 2at(\tfrac{1}{2}a)^2\right) = \tfrac{5}{3}a^3 t\,,$$

$$I_{\bar{z}\bar{z}} = \left(0 + 2at(\tfrac{1}{4}a)^2\right) + \left(\tfrac{1}{6}a^3 t + 2at(\tfrac{1}{4}a)^2\right) = \tfrac{5}{12}a^3 t\,,$$

$$I_{\bar{y}\bar{z}} = \left(0 + 2at\,(-\tfrac{1}{2}a)(-\tfrac{1}{4}a)\right) + \left(0 + 2at\,(\tfrac{1}{2}a)(\tfrac{1}{4}a)\right) = \tfrac{1}{2}a^3 t\,.$$

The first parenthesis represents the contribution from the horizontal flange, while the second represents the vertical flange. For the coupling moment of inertia $I_{\bar{y}\bar{z}}$ it is important to use the correct sign for the position of the local center with regard to the actual coordinate system. For the horizontal flange the local center C_1 is placed in the negative quadrant of the $\{\bar{y}, \bar{z}\}$ coordinate system, whereby both coordinates become negative. The contribution to $I_{\bar{y}\bar{z}}$ from the vertical flange 2 is also positive because the local center C_2 is located in the fully positive quadrant. □

Example 10.7. Moments of inertia for T-profile.

Figure 10.21 shows the thin-walled T-profile from Example 10.2. In this example the dimensions are chosen as follows:

$$a_w = a_f = a\,, \qquad E_w = E_f\,, \qquad t_w = \tfrac{1}{2}t_f = t\,.$$

By substitution of these relations into the expressions for the elastic center determined in Example 10.2 it is found that

$$c_y = 0\,, \qquad c_z = \tfrac{3}{16}a\,.$$

The coordinate system $\{\bar{y}, \bar{z}\}$ is placed with its origin in C, as shown in the figure.

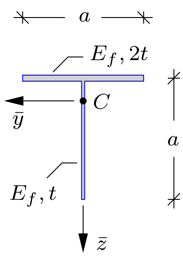

Fig. 10.21: Homogeneous T-profile.

The moments of inertia can now be determined by summation over the number of flanges following (10.45),

$$I_{\bar{y}\bar{y}} = \big(\tfrac{1}{12}a^3 2t + \tfrac{1}{12}t^3 a\big) = \tfrac{1}{6}\,a^3\,t\,,$$

$$I_{\bar{z}\bar{z}} = \big(\tfrac{1}{12}(2t)^3 a + 2at(\tfrac{3}{16}a)^2\big) + \big(\tfrac{1}{12}a^3 t + at\,(\tfrac{1}{2}a - \tfrac{3}{16}a)^2\big) = \tfrac{193}{768}\,a^3\,t \simeq 0.25\,a^3 t\,,$$

$$I_{\bar{y}\bar{z}} = 0 \quad \text{(symmetry)}\,.$$

The cross-section is assumed to be thin-walled, which implies that terms containing higher powers of thickness are omitted, whereby the only non-vanishing contribution to $I_{\bar{y}\bar{y}}$ given above is from the horizontal flange. Note also that the coupling moment of inertia is zero due to symmetry of the cross-section. □

Example 10.8. Moments of inertia for I-profile. Figure 10.22 shows an I-shaped cross-section. The flanges have dimensions $b \times t_f$ and elastic modulus E_f, while the web has dimensions $h \times t_w$ and elastic modulus E_w. Thus, the cross-section is inhomogeneous, and the reference elastic modulus is chosen as the flange value: $E_0 = E_f$. The particular geometry and material distribution implies that the cross-section is double symmetric and the elastic center is therefore located at the intersection of the lines of symmetry. In this case the origin of the reference coordinate system $\{y, z\}$ is therefore located directly at the elastic center.

Following (10.45) the moments of inertia are determined as

$$I_{yy} = \frac{1}{E_f}\big(E_w \tfrac{1}{12}t_w^3 h + 2E_f \tfrac{1}{12}b^3 t_f\big) = \tfrac{1}{6}b^3 t_f\,,$$

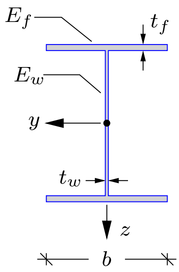

Fig. 10.22: Inhomogeneous thin-walled I-profile.

$$I_{zz} = \frac{1}{E_f}\Big(E_w \tfrac{1}{12} h^3 t_w + 2E_f\big(\tfrac{1}{12} t_f^3 b + bt_f(\tfrac{1}{2} h)^2\big)\Big) = \tfrac{1}{12}h^3 t_w \frac{E_w}{E_f} + \tfrac{1}{2}h^2 bt_f ,$$

$$I_{yz} = 0 \quad \text{(symmetry)} .$$

Again, terms containing higher powers of thickness are omitted, and the coupling moment of inertia is zero due to symmetry.

The moment of inertia with respect to the z-coordinate contains contributions from both web and flanges. In the simple case where $E_w = E_f$, $h = b = a$ and $t_w = t_f = t$ the two contributions reduce to

$$\tfrac{1}{12}h^3 t_w \frac{E_w}{E_f} = \tfrac{1}{12}a^3 t , \qquad \tfrac{1}{2}h^2 bt_f = \tfrac{1}{2}a^3 t .$$

This indicates that the main contribution to the bending stiffness of an I-profile with respect to the beam deformation in the z-direction comes from the flanges. Note furthermore that the relative contribution from the flanges increase with increasing height h of the cross-section. □

10.2.3 Principal coordinate system

By using a coordinate system with origin at the elastic center the problems of extension and bending uncouple and the constitutive relations appear in the separated form (10.40). The constitutive relations can be completely uncoupled by rotating the coordinate system $\{\bar{y}, \bar{z}\}$ until the coupling moment of inertia vanishes. The coordinate system in which the inertia matrix is diagonal is called the *principal coordinate system*, analogous to the use of the term in the context principal stresses and strains discussed in Chapter 8.

In Fig. 10.23 the coordinate system $\{\bar{y}, \bar{z}\}$ is rotated by the angle θ. Hereby the coordinates $[y', z']$ in the rotated system are obtained from the corresponding coordinates $[\bar{y}, \bar{z}]$ in the original coordinate system by the relation

$$\begin{bmatrix} y' \\ z' \end{bmatrix} = \begin{bmatrix} \cos\theta & \sin\theta \\ -\sin\theta & \cos\theta \end{bmatrix} \begin{bmatrix} \bar{y} \\ \bar{z} \end{bmatrix} , \tag{10.46}$$

with the inverse relation

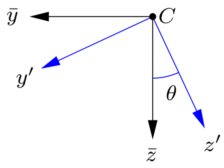

Fig. 10.23: Rotation of coordinate system.

$$\begin{bmatrix} \bar{y} \\ \bar{z} \end{bmatrix} = \begin{bmatrix} \cos\theta & -\sin\theta \\ \sin\theta & \cos\theta \end{bmatrix} \begin{bmatrix} y' \\ z' \end{bmatrix} . \tag{10.47}$$

Similar transform relations apply to other sets of vector components in the two coordinate systems, such as the inclinations $[\eta_y, \eta_z]$ with components $[\eta_{y'}, \eta_{z'}]$ in the rotated coordinate system.

The axial displacement field is given by (10.26) in the translated $\{\bar{y}, \bar{z}\}$ coordinate system, and when introducing the transforms (10.47) of both sets of components the following form is obtained

$$u = u_c + \bar{y}\,\eta_y + \bar{z}\,\eta_z = u_c + y'\,\eta_{y'} + z'\,\eta_{z'} . \tag{10.48}$$

The axial strain follows in a similar way from (10.27) as

$$\varepsilon = \varepsilon_c + \bar{y}\,\kappa_y + \bar{z}\,\kappa_z = \varepsilon_c + y'\,\kappa_{y'} + z'\,\kappa_{z'} , \tag{10.49}$$

with the axial strain at the elastic center C and the two curvatures defined as

$$\varepsilon_c = \frac{du_c}{dx} , \qquad \kappa_{y'} = \frac{d\eta_{y'}}{dx} , \qquad \kappa_{z'} = \frac{d\eta_{z'}}{dx} . \tag{10.50}$$

In fact, the relation (10.48) follows directly from the fact that the scalar product of two vectors is independent of the specific coordinate system used for the components.

The axial stress is obtained by multiplication of the axial strain with the elastic modulus, and the normal force is found by integration of the axial stress over the cross-section area,

$$N = \int_A E\varepsilon\, dA = E_0 F \varepsilon_c + E_0 S_{y'}\,\kappa_{y'} + E_0 S_{z'}\,\kappa_{z'} . \tag{10.51}$$

The static moments in the rotated coordinate system are obtained by substitution of (10.46) as

$$\begin{aligned} S_{y'} &= \frac{1}{E_0}\int_A E(\bar{y}\cos\theta + \bar{z}\sin\theta)\, dA &&= S_{\bar{y}}\cos\theta + S_{\bar{z}}\sin\theta = 0 , \\ S_{z'} &= \frac{1}{E_0}\int_A E(-\bar{y}\sin\theta + \bar{z}\cos\theta)\, dA &&= S_{\bar{y}}\cos\theta + S_{\bar{z}}\sin\theta = 0 , \end{aligned} \tag{10.52}$$

where the last equalities follow from the fact that static moments $S_{\bar{y}} = S_{\bar{z}} = 0$ in a coordinate system with origo at the elastic center. Thus, the constitutive relations in the rotated coordinate system have the form

$$N = E_0 F \varepsilon_c , \qquad \begin{bmatrix} M_{y'} \\ M_{z'} \end{bmatrix} = E_0 \begin{bmatrix} I_{y'y'} & I_{y'z'} \\ I_{y'z'} & I_{z'z'} \end{bmatrix} \begin{bmatrix} \kappa_{y'} \\ \kappa_{z'} \end{bmatrix} . \tag{10.53}$$

The moments of inertia in the rotated coordinate system are given as

$$\begin{aligned} I_{y'y'} &= \frac{1}{E_0} \int_A E y' y' \, dA = I_{\bar{y}\bar{y}} \cos^2\theta + I_{\bar{z}\bar{z}} \sin^2\theta + 2 I_{\bar{y}\bar{z}} \cos\theta \sin\theta , \\ I_{z'z'} &= \frac{1}{E_0} \int_A E z' z' \, dA = I_{\bar{y}\bar{y}} \sin^2\theta + I_{\bar{z}\bar{z}} \cos^2\theta - 2 I_{\bar{y}\bar{z}} \cos\theta \sin\theta , \\ I_{y'z'} &= \frac{1}{E_0} \int_A E y' z' \, dA = (I_{\bar{z}\bar{z}} - I_{\bar{y}\bar{y}}) \cos\theta \sin\theta + I_{\bar{y}\bar{z}} (\cos^2\theta - \sin^2\theta) , \end{aligned} \tag{10.54}$$

where the latter expressions are obtained by substitution of (10.46) followed by evaluation of the area integrals. The expressions in (10.54) are conveniently formulated in terms of the double angle, similar to the approach for stress components leading to the format in (8.68). Therefore, the following trigonometric relations are introduced,

$$2\cos\theta \sin\theta = \sin 2\theta , \qquad \cos^2\theta - \sin^2\theta = \cos 2\theta , \tag{10.55}$$

from which it follows that

$$\cos^2\theta = \tfrac{1}{2}\big(1 + \cos 2\theta \big) , \qquad \sin^2\theta = \tfrac{1}{2}\big(1 - \cos 2\theta \big) . \tag{10.56}$$

Hereby, the expressions (10.54) for the moments of inertia in the rotated coordinate system can be written as

$$\begin{aligned} I_{y'y'} &= \tfrac{1}{2}\big(I_{\bar{y}\bar{y}} + I_{\bar{z}\bar{z}} \big) + \tfrac{1}{2}\big(I_{\bar{y}\bar{y}} - I_{\bar{z}\bar{z}} \big) \cos 2\theta + I_{\bar{y}\bar{z}} \sin 2\theta , \\ I_{z'z'} &= \tfrac{1}{2}\big(I_{\bar{y}\bar{y}} + I_{\bar{z}\bar{z}} \big) - \tfrac{1}{2}\big(I_{\bar{y}\bar{y}} - I_{\bar{z}\bar{z}} \big) \cos 2\theta - I_{\bar{y}\bar{z}} \sin 2\theta , \\ I_{y'z'} &= \qquad\qquad\qquad\quad - \tfrac{1}{2}\big(I_{\bar{y}\bar{y}} - I_{\bar{z}\bar{z}} \big) \sin 2\theta + I_{\bar{y}\bar{z}} \cos 2\theta . \end{aligned} \tag{10.57}$$

The polar moment of inertia I_p is defined with respect to the distance from the elastic center, $r^2 = \bar{y}^2 + \bar{z}^2 = {y'}^2 + {z'}^2$, and thus

$$I_p = I_{\bar{y}\bar{y}} + I_{\bar{z}\bar{z}} = I_{y'y'} + I_{z'z'} . \tag{10.58}$$

It is seen that I_p, and thereby the sum of the diagonal moments of inertia, are invariant with respect to rotation of the coordinate system.

The bending splits into two uncoupled problems when the matrix is diagonal, and the new coordinate system is therefore rotated such that the coupling moment of inertia is zero,

$$I_{y'z'} \;=\; -\,\tfrac{1}{2}\big(I_{\bar{y}\bar{y}} - I_{\bar{z}\bar{z}}\big)\,\sin 2\theta \;+\; I_{\bar{y}\bar{z}}\,\cos 2\theta \;=\; 0\,. \tag{10.59}$$

This particular set of axes is called the *principal axes* of the cross-section. The equation (10.59) corresponds to

$$\tan 2\theta \;=\; \frac{2I_{\bar{y}\bar{z}}}{I_{\bar{y}\bar{y}} - I_{\bar{z}\bar{z}}}\,. \tag{10.60}$$

The angle can therefore be found as

$$\theta \;=\; \tfrac{1}{2}\arctan\left(\frac{2I_{\bar{y}\bar{z}}}{I_{\bar{y}\bar{y}} - I_{\bar{z}\bar{z}}}\right) \;+\; \tfrac{1}{2}\,n\pi\,, \tag{10.61}$$

where the second term takes the periodicity of the tangent function into account. If the angle θ_0 is the principal solution ($n = 0$) to (10.61) in the interval $-\frac{1}{2}\pi \le \theta_0 \le \frac{1}{2}\pi$, a second solution ($n = 1$) is given as $\theta_1 = \theta_0 + \frac{1}{2}\pi$ or $\theta_1 = \theta_0 + 90°$. Figure 10.24 illustrates the two orientations of the principal axes for an angle profile.

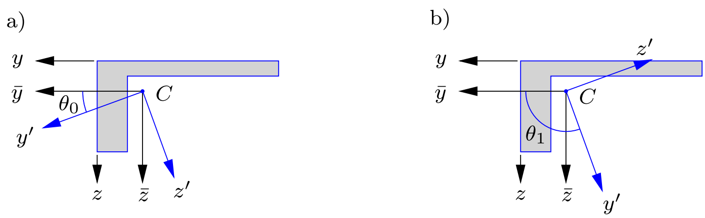

Fig. 10.24: Rotations of coordinate system.

In the coordinate system $\{y', z'\}$ the coupling moment of inertia vanishes, leaving only the two diagonal moments of inertia $I_{y'y'}$ and $I_{z'z'}$. The expression for these in terms of the original moments of inertia can be determined by the procedure used for stress components in Section 8.4.3 or by using the following relations for trigonometric functions of double angle,

$$\begin{aligned} \cos 2\theta &= \frac{\pm 1}{\sqrt{1+\tan^2 2\theta}} = \frac{\frac{1}{2}(I_{\bar{y}\bar{y}} - I_{\bar{z}\bar{z}})}{\sqrt{\frac{1}{4}(I_{\bar{y}\bar{y}} - I_{\bar{z}\bar{z}})^2 \,+\, I_{\bar{y}\bar{z}}^2}}\,, \\ \sin 2\theta &= \frac{\pm\tan 2\theta}{\sqrt{1+\tan^2 2\theta}} = \frac{I_{\bar{y}\bar{z}}}{\sqrt{\frac{1}{4}(I_{\bar{y}\bar{y}} - I_{\bar{z}\bar{z}})^2 \,+\, I_{\bar{y}\bar{z}}^2}}\,. \end{aligned} \tag{10.62}$$

By elimination of the trigonometric functions in (10.57) via the relations in (10.62) the moments of inertia with respect to the principal axes appear as

$$\left.\begin{matrix} I_{y'} \\ I_{z'} \end{matrix}\right\} = \frac{I_{\bar{y}\bar{y}} + I_{\bar{z}\bar{z}}}{2} \pm \sqrt{\left(\frac{I_{\bar{y}\bar{y}} - I_{\bar{z}\bar{z}}}{2}\right)^2 + I_{\bar{y}\bar{z}}^2}\,. \tag{10.63}$$

The plus sign represents the largest moment of inertia and the minus the smallest. The moments of inertia $I_{y'}$ and $I_{z'}$ with respect to the principal axes are denoted by a single subscript only, indicating that the coupling component is zero for this particular coordinate system orientation. Whether $I_{y'} > I_{z'}$ or $I_{z'} > I_{y'}$ depends on the choice of axes orientation. Figure 10.24a and b illustrate the rotation of the coordinate system by θ_0 and $\theta_1 = \theta_0 + \pi/2$, respectively. In the first case with θ_0 it is seen that $I_{y'} > I_{z'}$, whereby $I_{y'}$ is found by the plus in (10.63) and $I_{z'}$ by the minus. Conversely for θ_1, where it is seen that $I_{z'} > I_{y'}$, corresponding to $I_{z'}$ representing the plus in (10.63) and $I_{y'}$ the minus.

For cross-sections with symmetry with respect to one of the axes the coupling moment of inertia is already zero, and the axes therefore directly represent the principal coordinate system.

Principal values by eigenvalue problem

The principal moments of inertia of a cross-section can also be determined by an alternative strictly algebraic approach, similar to that used in Section 8.4.4 for three-dimensional states of stress. The principal directions are characterized by defining planes in which bending is uncoupled to bending out of the plane. Thus, if the components $[\kappa_{\bar{y}}, \kappa_{\bar{z}}]$ define curvatures in a principal plane, then the corresponding moment vector components $[M_{\bar{y}}, M_{\bar{z}}]$ will lie in the same plane. This property can be expressed by the relations

$$\begin{bmatrix} M_{\bar{y}} \\ M_{\bar{z}} \end{bmatrix} = E_0 \begin{bmatrix} I_{\bar{y}\bar{y}} & I_{\bar{y}\bar{z}} \\ I_{\bar{z}\bar{y}} & I_{\bar{z}\bar{z}} \end{bmatrix} \begin{bmatrix} \kappa_{\bar{y}} \\ \kappa_{\bar{z}} \end{bmatrix} = I\, E_0 \begin{bmatrix} \kappa_{\bar{y}} \\ \kappa_{\bar{z}} \end{bmatrix}, \tag{10.64}$$

where I is a proportionality factor representing the moment of inertia in the principal direction. The latter equality constitutes an eigenvalue problem of the form

$$\begin{bmatrix} I_{\bar{y}\bar{y}} - I & I_{\bar{y}\bar{z}} \\ I_{\bar{z}\bar{y}} & I_{\bar{z}\bar{z}} - I \end{bmatrix} \begin{bmatrix} \kappa_{\bar{y}} \\ \kappa_{\bar{z}} \end{bmatrix} = \begin{bmatrix} 0 \\ 0 \end{bmatrix}, \tag{10.65}$$

where the moment of inertia I appears as the eigenvalue, while the eigenvector $[\kappa_{\bar{y}}, \kappa_{\bar{z}}]$ defines the principal curvature direction. The equations (10.65) are homogeneous and the existence of non-trivial solutions requires the determinant of the matrix to vanish. This provides the characteristic equation

$$(I_{\bar{y}\bar{y}} - I)(I_{\bar{z}\bar{z}} - I) - I_{\bar{y}\bar{z}}^2 = 0\,. \tag{10.66}$$

This is a quadratic equation in the eigenvalue I,

$$I^2 - (I_{\bar{y}\bar{y}} + I_{\bar{z}\bar{z}})\,I + (I_{\bar{y}\bar{y}}I_{\bar{z}\bar{z}} - I_{\bar{y}\bar{z}}^2) = 0\,. \tag{10.67}$$

The solutions to this equation are similar to the expressions for the principal moments of inertia already derived by different means in (10.63),

$$\left.\begin{matrix} I_{y'} \\ I_{z'} \end{matrix}\right\} = \frac{I_{\bar{y}\bar{y}} + I_{\bar{z}\bar{z}}}{2} \pm \sqrt{\left(\frac{I_{\bar{y}\bar{y}} - I_{\bar{z}\bar{z}}}{2}\right)^2 + I_{\bar{y}\bar{z}}^2}\,. \tag{10.68}$$

The eigenvalue formulation is well suited to numerical solution, providing the principal moments of inertia as eigenvalues, and the principal directions via the eigenvectors.

Example 10.9. Principal properties of angle profile. Figure 10.25 shows the angle profile previously considered in Example 10.1, where the position of the elastic center was determined, and Example 10.6, where the corresponding moments of inertia were obtained as,

$$I_{\bar{y}\bar{y}} = \tfrac{5}{3}a^3t\,, \qquad I_{\bar{z}\bar{z}} = \tfrac{5}{12}a^3t\,, \qquad I_{\bar{y}\bar{z}} = \tfrac{1}{2}a^3t\,.$$

Note that $I_{\bar{y}\bar{z}} \neq 0$, and thus the $\{\bar{y}, \bar{z}\}$ axes are not the principal axes.

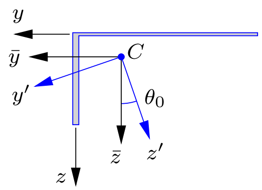

Fig. 10.25: Homogeneous thin-walled angle profile.

The counterclockwise angle of rotation of the principal coordinate system $\{y', z'\}$ relative to the $\{\bar{y}, \bar{z}\}$ coordinate system is given by (10.60),

$$\tan 2\theta = \frac{2I_{\bar{y}\bar{z}}}{I_{\bar{y}\bar{y}} - I_{\bar{z}\bar{z}}} = \frac{2\,\frac{1}{2}\,a^3t}{\frac{5}{3}\,a^3t - \frac{5}{12}a^3t} = \tfrac{4}{5}\,.$$

Thus the angle is

$$\theta_0 = 19.3^\circ$$

where subscript 0 indicates that the result corresponds to the principal value of the tangent function with $n = 0$. The orientation of the principal axes $\{y', z'\}$ is shown in Fig. 10.25.

The principal moments of inertia are given by the expressions in (10.63),

$$\left.\begin{matrix} I_{y'} \\ I_{z'} \end{matrix}\right\} = \left(\frac{25}{24} \pm \frac{\sqrt{41}}{8}\right) a^3t\,.$$

With respect to the definition of the $\{y', z'\}$ axes it is seen that $I_{y'} > I_{z'}$, which means that $I_{y'}$ corresponds to the plus in the expression above, while $I_{z'}$ corresponds to the minus:

$$I_{y'} = 1.84\,a^3t\,, \qquad I_{z'} = 0.24\,a^3t\,.$$

In the case of $\theta = \theta + 90^\circ = 109.3^\circ$ these values would be interchanged. □

Example 10.10. Principal properties of Z-profile. Figure 10.26 shows a Z-profile with constant thickness t, height $2a$ and width $2a$. The specific dimensions are given in the figure. The cross-section has point symmetry about C, which is therefore the elastic center, as indicated in the figure. The coordinate axes $\{y, z\}$ are parallel to the flanges and web, respectively, and with origin at the elastic center. The cross-section is homogeneous, whereby the elastic modulus cancels in the expression for the moments of inertia. The cross-section is assumed to be thin-walled with $t \ll a$.

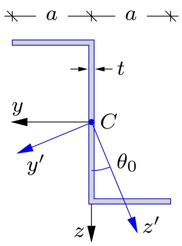

Fig. 10.26: Homogeneous Z-profile.

The moments of inertia with respect to the $\{y, z\}$ axes are determined as

$$I_{yy} = 2\left(\tfrac{1}{12}a^3t + at(\tfrac{1}{2}a)^2\right) = \tfrac{2}{3}a^3t\,,$$

$$I_{zz} = \tfrac{1}{12}(2a)^3t + 2ata^2 = \tfrac{8}{3}a^3t\,,$$

$$I_{yz} = at\,a\left(-\tfrac{1}{2}a\right) + at(-a)\,\tfrac{1}{2}a = -a^3t\,,$$

where terms containing higher powers in t are omitted. The coupling moment of inertia $I_{yz} \neq 0$ and thus $\{y, z\}$ are not principal axes. The orientation of the principal axes $\{y', z'\}$ is governed by the angle θ determined by (10.60) and (10.61),

$$\tan(2\theta) = 1 \qquad \Rightarrow \qquad \theta_n = 22.5^\circ + n\,90^\circ\,.$$

For $n = 0$ the angle is $\theta_0 = 22.5^\circ$, and the orientation of the principal axes for this angle is shown in Fig. 10.26.

The principal moments of inertia are determined by the expressions in (10.63),

$$\left.\begin{matrix} I_{y'} \\ I_{z'} \end{matrix}\right\} = \left(\tfrac{5}{3} \pm \sqrt{2}\right)a^3t\,.$$

From Fig. 10.26 it is seen that $I_{z'} > I_{y'}$, corresponding to

$$I_{y'} = \left(\tfrac{5}{3} - \sqrt{2}\right)a^3t = 0.25\,a^3t\,, \qquad I_{z'} = \left(\tfrac{5}{3} + \sqrt{2}\right)a^3t = 3.08\,a^3t\,.$$

The largest moment of inertia in the principal directions is larger than the moments of inertia in the original $\{y, z\}$ axes. Thus, for non-symmetric cross-sections the principal directions indicate the optimal orientation of the cross-section with respect to unidirectional transverse loading. This relates to the concept of Mohr's circle, as discussed next. □

Mohr's circle for moments of inertia

The transformation relations for moments of inertia in a rotated coordinate system (10.57) and the associated expression (10.63) for the principal moments of inertia are similar to the transformation relations (8.68) in plane stress and the expression (8.80) for the associated principal stresses. This indicates that the moments of inertia $I_{y'y'}$, $I_{z'z'}$ and $I_{y'z'}$ can be illustrated graphically by the Mohr's circle construction in terms of the principal moments of inertia.

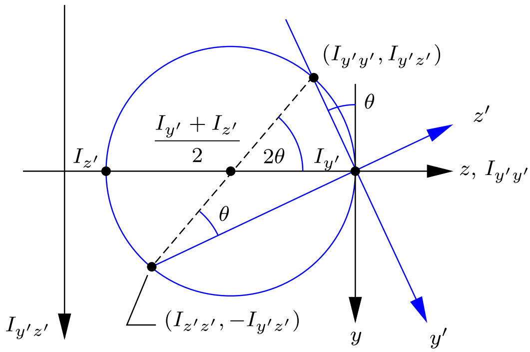

Fig. 10.27: Mohr's circle in the $(I_{y'y'}, I_{y'z'})$-plane with $I_{y'} > I_{z'}$.

Let $\{\bar{y}, \bar{z}\}$ take the role of the principal coordinate system with the principal moments of inertia $I_{y'}$ and $I_{z'}$. The moments of inertia in a coordinate system $\{y', z'\}$, obtained by a counter clockwise rotation θ, is then obtained from the transformation relations (10.57) as

$$\begin{aligned} I_{y'y'} &= \tfrac{1}{2}\big(I_{y'} + I_{z'}\big) + \tfrac{1}{2}\big(I_{y'} - I_{z'}\big)\cos 2\theta\,, \\ I_{z'z'} &= \tfrac{1}{2}\big(I_{y'} + I_{z'}\big) - \tfrac{1}{2}\big(I_{y'} - I_{z'}\big)\cos 2\theta\,, \\ I_{y'z'} &= \qquad\qquad\qquad - \tfrac{1}{2}\big(I_{y'} - I_{z'}\big)\sin 2\theta\,. \end{aligned} \tag{10.69}$$

The moments of inertia $I_{y'y'}$, $I_{z'z'}$ and $I_{y'z'}$ can now be illustrated graphically as a function of the angle θ as shown in Fig. 10.27. Let $I_{y'y'}$ serve as horizontal axis and $I_{y'z'}$ as vertical downward axis. The relations (10.69a) and (10.69c) constitute a parameter representation by which the point $[I_{y'y'}, I_{y'z'}]$ moves around in the counter clockwise direction as described by the center angle 2θ. The center of the circle is located at the horizontal axis,

$$C = [c, 0]\,, \quad c = \tfrac{1}{2}\big(I_{y'} + I_{z'}\big)\,, \tag{10.70}$$

and the radius is

$$R = \tfrac{1}{2}\big|I_{y'} - I_{z'}\big|. \tag{10.71}$$

It follows from the relations (10.69b) and (10.69c) that $[I_{z'z'}, -I_{y'z'}]$ is the diametrically opposite point on the circle. It is clear from this construction that the principal moments of inertia $I_{y'}$ and $I_{z'}$ constitute the maximum and minimum values of $I_{y'y'}$ and $I_{z'z'}$. These results correspond to those obtained for the plane stress components in (8.84).

Example 10.11. Mohr's circle for angle profile. Consider the angle profile in Fig. 10.25, where the original axes are now denoted $\{y', z'\}$ to indicate a non-principal coordinate system. The moments of inertia are

$$I_{y'y'} = \tfrac{5}{3}a^3t\,, \qquad I_{z'z'} = \tfrac{5}{12}a^3t\,, \qquad I_{y'z'} = \tfrac{1}{2}a^3t\,.$$

In Fig. 10.28 these values identify the two points $[I_{y'y'}, I_{y'z'}]$ and $[I_{z'z'}, -I_{y'z'}]$, shown in the figure normalized by $\frac{1}{12}a^3t$. The two points identify the center $c = \frac{1}{2}(\frac{5}{3} + \frac{5}{12})a^3t = \frac{25}{24}a^3t$ and thereby the radius. Alternatively, the circle may be constructed from the principal values

$$I_{y'} = 1.84\,a^3t\,, \qquad I_{z'} = 0.24\,a^3t\,,$$

obtained in Example 10.9. □

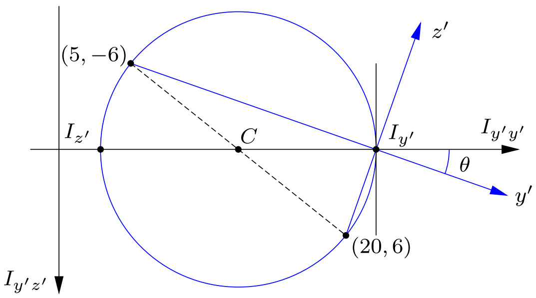

Fig. 10.28: Mohr's circle in $(I_{y'y'}, I_{y'z'})$-plane for angle profile.

10.3 Axial stresses and strains

In the general $\{y, z\}$ coordinate system the axial strain ε is given by (10.3) and the associated axial stress σ is found by multiplication with the elastic modulus E, as shown in (10.10). Both the strain and the stress distributions are functions of the deformation measures ε_0, κ_y and κ_z, as shown in Fig. 10.5. They are given in terms of the internal forces N, M_y and M_z with respect to the $\{y, z\}$ coordinate system by the general constitutive relation in (10.21). This requires inversion of the 3×3 stiffness matrix in (10.21), whereby the axial strain can be written as

$$\varepsilon = [1, y, z]\begin{bmatrix}\varepsilon_0\\ \kappa_y\\ \kappa_z\end{bmatrix} = \frac{1}{E_0}[1, y, z]\begin{bmatrix}F & S_y & S_z\\ S_y & I_{yy} & I_{yz}\\ S_z & I_{yz} & I_{zz}\end{bmatrix}^{-1}\begin{bmatrix}N\\ M_y\\ M_z\end{bmatrix}. \qquad (10.72)$$

This procedure often requires numerical tools because of the inversion of the general cross-section stiffness matrix. The stress distribution is then obtained by multiplication with the elastic modulus,

$$\sigma = E\varepsilon. \qquad (10.73)$$

The kinematic formulation implies a linear strain distribution, as shown in Fig. 10.3, and for homogeneous cross-sections the associated stress distribution is linear as well. However, for inhomogeneous cross-sections discontinuities may occur in the stress distribution due to sudden changes in the elastic modulus. Therefore, the basis of any stress analysis is the determination of the associated continuous strain distribution.

Separation of extension and bending

For analytical calculations it is convenient to separate the extension and bending problems by describing the axial strain and stress with respect to the (translated) coordinate system $\{\bar{y}, \bar{z}\}$ with origin at the elastic center. In that case the contributions to the axial deformation from pure extension and bending are separated, as illustrated in Fig. 10.8. The constitutive relations are given in (10.40) and the axial strain can be written as

$$\varepsilon(y,z) = \varepsilon_c + [\bar{y}, \bar{z}]\begin{bmatrix}\kappa_y\\ \kappa_z\end{bmatrix}, \qquad (10.74)$$

where the extension and the bending problems are separated and appear in an additive format. Elimination of the deformation measures ε_c, κ_y and κ_z by the constitutive relations (10.40) gives the following expression for the axial strain in terms of the internal forces with respect to the $\{\bar{y}, \bar{z}\}$ coordinate system,

$$\varepsilon(y,z) = \frac{1}{E_0}\left(\frac{N}{F} + [\bar{y}, \bar{z}]\begin{bmatrix}I_{\bar{y}\bar{y}} & I_{\bar{y}\bar{z}}\\ I_{\bar{y}\bar{z}} & I_{\bar{z}\bar{z}}\end{bmatrix}^{-1}\begin{bmatrix}M_{\bar{y}}\\ M_{\bar{z}}\end{bmatrix}\right). \qquad (10.75)$$

The inverse of the 2×2 bending stiffness matrix can be written in explicit form as

$$\begin{bmatrix}I_{\bar{y}\bar{y}} & I_{\bar{y}\bar{z}}\\ I_{\bar{y}\bar{z}} & I_{\bar{z}\bar{z}}\end{bmatrix}^{-1} = \frac{1}{I_{\bar{y}\bar{y}}I_{\bar{z}\bar{z}} - I_{\bar{y}\bar{z}}^2}\begin{bmatrix}I_{\bar{z}\bar{z}} & -I_{\bar{y}\bar{z}}\\ -I_{\bar{y}\bar{z}} & I_{\bar{y}\bar{y}}\end{bmatrix}, \qquad (10.76)$$

where the denominator of the fraction is the determinant of the 2×2 bending moment of inertia matrix. The stress distribution is found by multiplication

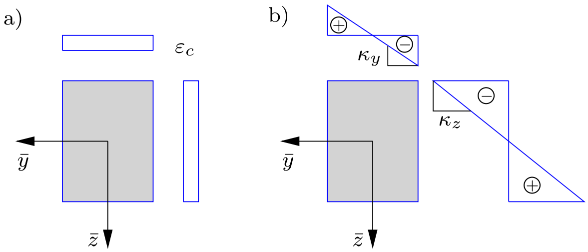

Fig. 10.29: Plot of linear strain variation: a) extension, and b) bending.

with the elastic modulus, as in (10.73). The separation of the strain distribution into contributions from extension and bending is illustrated in Fig. 10.29, where it is indicated that the strain contribution from bending, governed by the second term in (10.75), vanishes at the elastic center. The resulting strain distribution is the sum of the two contributions, as demonstrated by the expression in (10.75).

Example 10.12. Axial stress in cantilever with angle profile. Figure 10.30 shows a cantilever of length ℓ with tip loads P in the y direction and $\frac{1}{2}P$ in the z direction. The present example determines the axial stress at the fixed support, where the moments are:

$$M_y = -Pl\,, \qquad M_z = -\tfrac{1}{2}\,Pl\,.$$

Note, that the moments are negative following the sign convention introduced in Chapter 3. The cross-section of the cantilever is the angle profile shown in Fig. 10.31. The location of the elastic center has been determined in Example 10.1, and in the present case the coordinate system $\{y,z\}$ is located with origin at the elastic center. The precise location of the transverse force in the cross-section plane that does not introduce torsion depends on the shear stress distribution and is dealt with in Chapter 11.

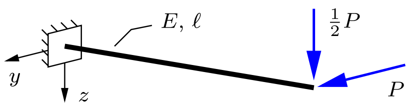

Fig. 10.30: Cantilever with tip loads P and $\frac{1}{2}P$.

The axial strain is given by the relation in (10.75). This expression involves the inverse of the bending stiffness matrix given in (10.76). For the angle profile the moments of inertia have been found in Example 10.6,

$$I_{yy} = \tfrac{5}{3}a^3t\,, \qquad I_{zz} = \tfrac{5}{12}a^3t\,, \qquad I_{yz} = \tfrac{1}{2}a^3t\,,$$

and the inverse matrix is

$$\begin{bmatrix} I_{yy} & I_{yz} \\ I_{yz} & I_{zz} \end{bmatrix}^{-1} = \frac{3}{16}\begin{bmatrix} 5 & -6 \\ -6 & 20 \end{bmatrix}\frac{1}{a^3t}\,.$$

The expression for the axial strain is given in (10.75). In the present example it leads to

$$\varepsilon(y,z) = -\frac{1}{E_0}\frac{3}{16}[\,y\,,\,z\,]\begin{bmatrix} 5 & -6 \\ -6 & 20 \end{bmatrix}\begin{bmatrix} 1 \\ \frac{1}{2} \end{bmatrix}\frac{P\ell}{a^3 t} = -\frac{3}{8}\frac{P\ell}{E_0 a^3 t}(y+2z)\,,$$

where the minus follows from the negative bending moments M_y and M_z.

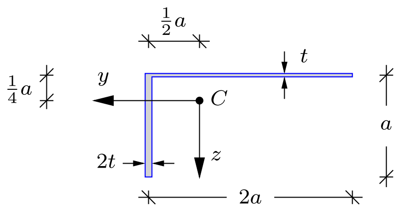

Fig. 10.31: Homogeneous thin-walled angle profile.

The linear axial strain distribution is plotted along the coordinate axes in Fig. 10.32. Along the y-axis, with $z = 0$, the strain variation is

$$\varepsilon(y,0) = -\frac{3}{8}\,y\,\frac{P\ell}{E_0 a^2 t}\,,$$

and along the z-axis, with $y = 0$, it is

$$\varepsilon(0,z) = -\frac{3}{4}\,z\,\frac{P\ell}{E_0 a^2 t}\,.$$

These linear variations of the axial strain along the two coordinate axes is shown in Fig. 10.32. The values given in the figure correspond to the normalized strain $\varepsilon\, E_0\, a^2 t/(P\ell)$. The corresponding stress variations are found by multiplication with $E = E_0$.

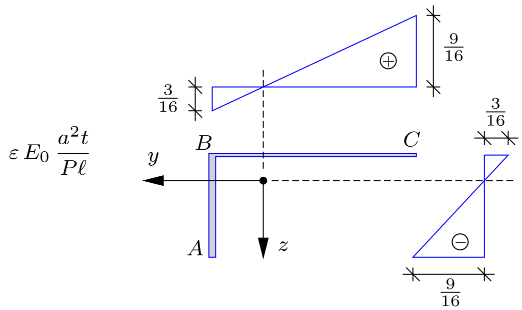

Fig. 10.32: Variation of normalized strain along coordinate axes.

The variations of the strain along the coordinate axes can be used to determine the strain and stress at end and corner points of the cross-section, which are denoted as points A, B and C in Fig. 10.32. The stress in A is found as

$$\sigma_A = E_0\,\varepsilon_A = -\Big(\frac{3}{16} + \frac{9}{16}\Big)\frac{P\ell}{a^2 t} = -\frac{3}{4}\frac{P\ell}{a^2 t}\,.$$

This result can be verified by substitution of $y = \frac{1}{2}a$ and $z = \frac{3}{4}a$ into the expression for $\varepsilon(y,z)$ given previously,

$$\sigma_A = E_0\,\varepsilon\big(\tfrac{1}{2}\,a,\,\tfrac{3}{4}\,a\big) = -\frac{3}{8}\,\frac{P\ell}{E_0 a^3 t}\,\big(\tfrac{1}{2}a + \tfrac{3}{2}a\big) = -\frac{3}{4}\,\frac{P\ell}{a^2 t}\,.$$

Similarly, the stress in B and C can be determined by combination of the axis values given in Fig. 10.32, or by substitution of the coordinates into the general expression for the strain. It is often convenient to set up a table containing the strains and stresses at end and corner points of the cross-section. In the present case the stress distribution is fully determined by the values in A, B and C, which are given in Table 10.1.

Table 10.1: Axial stress in angle profile.

point	y	z	$\sigma\,\dfrac{a^2t}{P\ell}$
A	$\frac{1}{2}\,a$	$\frac{3}{4}\,a$	$-\frac{3}{4}$
B	$\frac{1}{2}\,a$	$-\frac{1}{4}\,a$	0
C	$-\frac{3}{2}\,a$	$-\frac{1}{4}\,a$	$\frac{3}{4}$

The axial stress can also be plotted along the contour of the cross-section, as shown in Fig. 10.33, using the linear variation along straight parts of the contour.

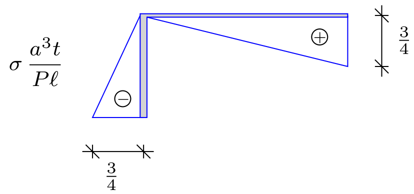

Fig. 10.33: Axial stress distribution along cross-section contour.

The particular loading of the cantilever yields zero stress at the corner B, while the maximum stresses are present at the end points A and B. Assume that σ_Y is the yield stress in the von Mises yield condition. The maximum force P associated with this yield stress is then found as

$$P_{\max} = \pm\,\frac{4}{3}\,\frac{a^3 t}{\ell}\,\sigma_Y\,.$$

Note, that because the shear stress is omitted here the Tresca failure condition gives the same yield limit. □

Example 10.13. Stresses in simply supported beam with Z-profile. Figure 10.34a shows a simply supported beam with distributed load in the z direction with constant intensity p. The present example determines the axial strain and stress from bending at the center of the span in C, where the moments are

$$M_y^C = 0\,, \qquad M_z^C = \tfrac{1}{8}p\ell^2\,.$$

The beam is homogeneous with elastic modulus $E = E_0$, and the cross-section is the Z-profile shown in Fig. 10.34b. The moments of inertia of this cross-section have been

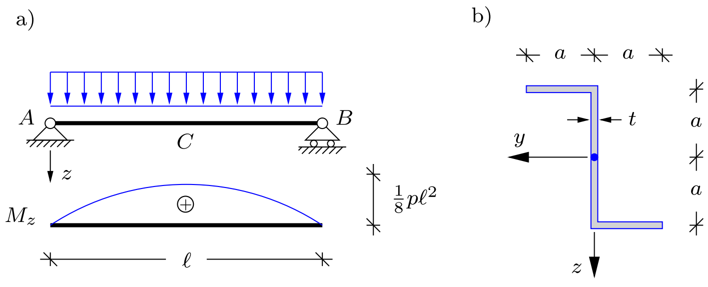

Fig. 10.34: Simply supported beam with distributed load.

determined in Example 10.10,

$$I_{yy} = \tfrac{2}{3}a^3t\,, \qquad I_{zz} = \tfrac{8}{3}a^3t\,, \qquad I_{yz} = -a^3t\,.$$

The inverse of the bending stiffness matrix is

$$\begin{bmatrix} I_{yy} & I_{yz} \\ I_{yz} & I_{zz} \end{bmatrix}^{-1} = \frac{3}{7}\begin{bmatrix} 8 & 3 \\ 3 & 2 \end{bmatrix}\frac{1}{a^3t}\,,$$

and the strain distribution is then obtained by (10.75),

$$\varepsilon(y,z) = \frac{1}{E_0}\,\frac{3}{56}\,[\,y\,,\,z\,]\begin{bmatrix} 8 & 3 \\ 3 & 2 \end{bmatrix}\begin{bmatrix} 0 \\ 1 \end{bmatrix}\frac{p\ell^2}{a^3t} = \frac{3}{56}\,\frac{p\ell^2}{E_0a^3t}\,(3y+2z)\,.$$

The strain distribution is shown in Fig. 10.35a with respect to the coordinate axes.

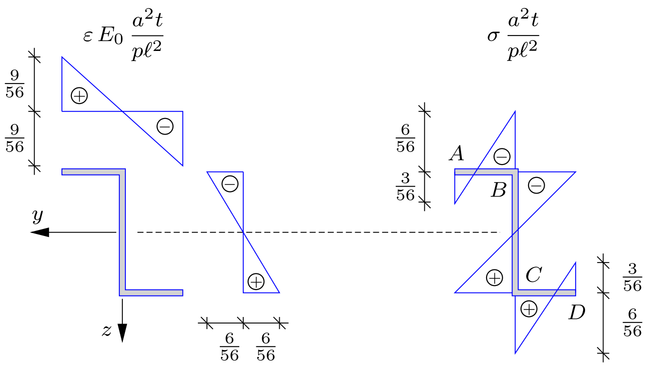

Fig. 10.35: a) Strain and b) stress distribution.

The stress distribution is obtained by multiplication with the elastic modulus, which is constant $E = E_0$ for the present homogeneous beam. The value of the axial stress is found at the ends and corners A to D of the profile as shown in Fig. 10.35b. In A the axial stress σ_A is found by superposition of the strain distribution in Fig. 10.35a,

$$\sigma_A = E_0\,\varepsilon_A = \left(\frac{9}{56} - \frac{6}{56}\right)\frac{p\ell^2}{a^2t} = \frac{3}{56}\,\frac{p\ell^2}{a^2t}\,.$$

Table 10.2: Axial stress in angle profile.

point	y	z	$\sigma \dfrac{a^2 t}{p\ell^2}$
A	a	$-a$	$\frac{3}{56}$
B	0	$-a$	$-\frac{6}{56}$
C	0	a	$\frac{6}{56}$
D	$-a$	a	$-\frac{3}{56}$

Table 10.2 gives the axial stress at the four points on the cross-section. The full stress distribution is obtained by linear interpolation between the four values, as shown in Fig. 10.35b. The maximum axial stress occurs in points B and C, with $\sigma_{\max} = \pm\frac{6}{56}p\ell^2/(a^2t)$. □

Principal axes

In the principal coordinate system the coupling moment of inertia $I_{y'z'} = 0$, whereby the bending stiffness matrix becomes diagonal. The constitutive relations are hereby given as

$$N = E_0 F\,\varepsilon_c\,, \qquad M_{y'} = E_0 I_{y'}\kappa_{y'}\,, \qquad M_{z'} = E_0 I_{z'}\kappa_{z'}\,. \tag{10.77}$$

The axial strain in the principal coordinate system is defined in (10.48). Elimination of axial strain and curvatures in terms of the section forces yields

$$\varepsilon = \frac{1}{E_0}\left(\frac{N}{F} + \frac{M_{y'}}{I_{y'}}\,y' + \frac{M_{z'}}{I_{z'}}\,z'\right). \tag{10.78}$$

The associated stress distribution is obtained by multiplication with the elastic modulus

$$\sigma = \frac{E}{E_0}\left(\frac{N}{F} + \frac{M_{y'}}{I_{y'}}\,y' + \frac{M_{z'}}{I_{z'}}\,z'\right). \tag{10.79}$$

The stress distribution expressed via the linear kinematic formulation and in terms of section forces is often referred to as the Navier stress distribution.

Example 10.14. Axial stresses in cantilever with I-profile. Figure 10.36a shows a cantilever loaded by a tip force P acting in the z direction. The beam is homogeneous with elastic modulus $E_0 = E$ and length ℓ. The distribution of strain and stress is determined at the fixed support, where the bending moment attains its maximum,

$$M_z = -P\ell\,.$$

The cross-section is an I-profile with height and width a and thickness t, as shown in Fig. 10.36b.

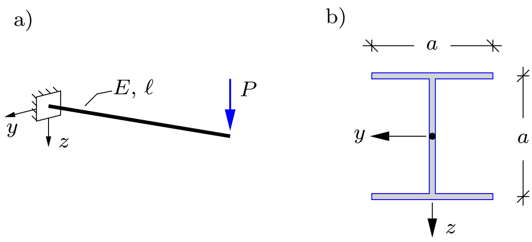

Fig. 10.36: a) Cantilever with tip load P, and b) I-profile cross-section.

The cross-section has double symmetry with respect to the coordinate system shown in the figure, which hereby is a principal coordinate system. Thus, the strain distribution is determined by the simplified expression (10.78). Since $N = 0$ and $M_y = 0$ this expression reduces to

$$\varepsilon = \frac{1}{E}\frac{M_z}{I_z}z\,.$$

The moment of inertia with respect to the z-direction is

$$I_z = \tfrac{1}{12}a^3t + 2at\big(\tfrac{1}{2}\,a\big)^2 = \big(\tfrac{1}{12}+\tfrac{1}{2}\big)a^3t = \tfrac{7}{12}\,a^3\,t\,.$$

This agrees with the result obtained in Example 10.8 for the inhomogeneous I-profile. The expression for the axial strain is now determined as

$$\varepsilon = -\frac{1}{E}\frac{12}{7}\frac{P\ell}{a^3t}\,z\,.$$

The corresponding axial stress is found by multiplication of the strain with the constant elastic modulus E, and thus the strain and stress distribution are similar in shape. Figure 10.37a shows the variation of the axial strain along the z-axis, whereas in Fig. 10.37b the axial stress is plotted along the center lines of the thin-walled cross-section. The negative strain and stress indicates that the bottom flange is in compression, in agreement with the negative sign of the bending moment M_z. □

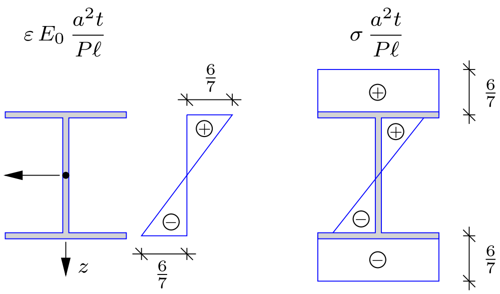

Fig. 10.37: Normalized distributions of axial strain and stress.

Example 10.15. Inhomogeneous I-profile. This example considers the inhomogeneous I-profile cross-section shown in Fig. 10.38. As in the previous example the beam is loaded by a transverse force P in the z-direction, producing the moment

$$M_z = -P\ell\,.$$

The height and width of the cross-section is a, the thickness of the flanges is t, while the thickness of the web is only $\frac{1}{5}t$. The elastic modulus of the flanges is E_f, while the web has elastic modulus $E_w = 5E_f$. In the following the reference elastic modulus is chosen as the flange value, $E_0 = E_f$.

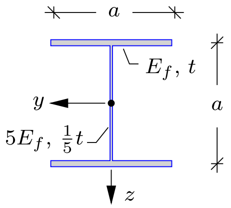

Fig. 10.38: Inhomogeneous I-profile cross-section.

The continuous strain distribution is determined by (10.78),

$$\varepsilon \,=\, \frac{1}{E_0}\,\frac{M_z}{I_z}\,z\,.$$

The moment of inertia in the z-direction is determined as

$$I_z \,=\, \frac{E_w}{E_f}\,\tfrac{1}{12}\,a^3\,\tfrac{1}{5}t \,+\, 2\,at\left(\tfrac{1}{2}\,a\right)^2 \,=\, \tfrac{7}{12}\,a^3\,t\,,$$

which by design is equal to the moment of inertia for the homogeneous cross-section in the previous example. Substitution into the strain expression gives

$$\varepsilon \,=\, -\,\frac{1}{E_f}\,\frac{12}{7}\,\frac{P\ell}{a^3 t}\,z\,.$$

The linear variation of the strain ε along the z-direction is shown in Fig. 10.39a. The stress distribution is obtained by multiplication of the strain by the elastic modulus. Since the cross-section is inhomogeneous with different elastic moduli, discontinuities in the stress variation occur. Table 10.3 gives the strain and the associated stress values at the points A and D located in the flanges, and B and C located at the top and bottom of the web, as shown in Fig. 10.39. It is seen that the stresses in the web are significantly larger due to the large elastic modulus. The stress distribution is also shown in Fig. 10.39b.

Assume that the yield stress of the flange material is $\sigma_Y = \sigma_f$, while it is $\sigma_Y = 10\sigma_f$ for the web material. In the present case the only stress component is the axial stress σ,

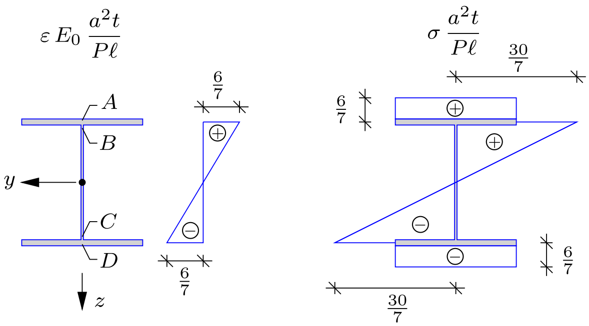

Fig. 10.39: Normalized distributions of axial strain and stress for inhomogeneous I-profile.

Table 10.3: Axial stress in angle profile.

point	y	z	$\varepsilon\, E_f\, \dfrac{a^2 t}{P\ell}$	$\sigma\, \dfrac{a^2 t}{P\ell}$
A	$-\frac{1}{2}\,a$	0	$\frac{6}{7}$	$\frac{6}{7}$
B	$-\frac{1}{2}\,a$	0	$\frac{6}{7}$	$\frac{30}{7}$
C	$\frac{1}{2}\,a$	0	$-\frac{6}{7}$	$-\frac{30}{7}$
D	$\frac{1}{2}\,a$	0	$-\frac{6}{7}$	$-\frac{6}{7}$

whereby the von Mises yield condition (9.57) gives $\sigma = \sigma_Y$. For the flanges the maximum stress is $\pm\frac{6}{7}P\ell/(a^2 t)$, which for $\sigma_Y = \sigma_f$ gives the yield load

$$P^f_{\max} \,=\, \frac{7}{6}\,\frac{a^2 t}{\ell}\,\sigma_f\,.$$

Thus, failure occurs in the flanges when the load P reaches $P^f_{\max}$. The maximum stress in the web is $\pm\frac{30}{7}P\ell/(a^2 t)$, and failure occurs when this value reaches $10\sigma_f$. This gives

$$P^w_{\max} \,=\, \frac{7}{3}\,\frac{a^2 t}{\ell}\,\sigma_f \,>\, P^f_{\max}\,.$$

This shows that although the stresses in the web are larger than those in the flanges, the significantly smaller yield stress of the flange material implies that it is in fact the flanges that limit the maximum loading of the beam by $P_{\max} = P^f_{\max}$. □

10.3.1 Neutral axis and line of curvature

A number of materials, such as concrete, have significantly larger strength in compression than in tension. For beams composed of this type of material it is therefore of interest to determine the regions of the cross-section that are in compression and tension, respectively. The linear form of the strain distribution implies that the transition between the compression and tension regions is described by a straight line, typically denoted as the *neutral axis.* In the coordinate system with the elastic center as origin the axial strain is given by (10.27). Thus, the neutral axis is given by the relation

$$\varepsilon_c \,+\, \bar{y}\,\kappa_y \,+\, \bar{z}\,\kappa_z \,=\, 0\,, \tag{10.80}$$

where the curvature is given in terms of the bending moments by the constitutive relation (10.40b). The straight line representing the neutral axis is fixed by two points. These are conveniently chosen as the intersections with the y and z axes, respectively. It follows from (10.80) that

$$\begin{aligned} \bar{y}_n &= -\,\frac{\varepsilon_c}{\kappa_y} \qquad \text{for} \qquad z \,=\, 0\,, \\ \bar{z}_n &= -\,\frac{\varepsilon_c}{\kappa_z} \qquad \text{for} \qquad y \,=\, 0\,, \end{aligned} \tag{10.81}$$

where the subscript n indicates that these points define the intersections of the coordinate axes with the neutral axis. For pure bending $\varepsilon_c = 0$, and the neutral axis passes through the elastic center C.

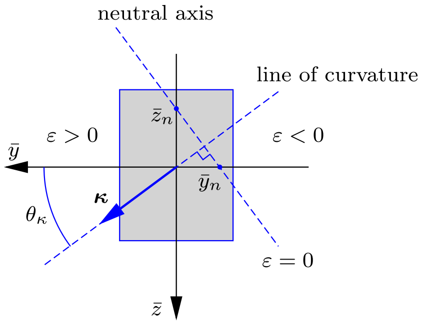

Fig. 10.40: Neutral axis perpendicular to line of curvature.

The direction of the neutral axis in the cross-section plane is determined by the two curvature terms in (10.80). When considering the coordinate increments $[d\bar{y}, d\bar{z}]$ along the neutral axis, it follows from differentiation of (10.80) that these satisfy the equation

$$[d\bar{y}, d\bar{z}] \begin{bmatrix} \kappa_y \\ \kappa_z \end{bmatrix} = 0\,. \tag{10.82}$$

It follows from this relation that the direction of the neutral axis $[d\bar{y}, d\bar{z}]$ is perpendicular to the curvature vector $[\kappa_y, \kappa_z]$. In a coordinate system with the elastic center as origin the curvature vector components are given in terms of the moment vector components as

$$\begin{bmatrix} \kappa_y \\ \kappa_z \end{bmatrix} = \frac{1}{E_0} \begin{bmatrix} I_{\bar{y}\bar{y}} & I_{\bar{y}\bar{z}} \\ I_{\bar{y}\bar{z}} & I_{\bar{z}\bar{z}} \end{bmatrix}^{-1} \begin{bmatrix} M_{\bar{y}} \\ M_{\bar{z}} \end{bmatrix}. \tag{10.83}$$

The axial strain at the elastic center ε_c is simply an offset of the neutral axis along the normal.

In Fig. 10.40 the curvature vector $\boldsymbol{\kappa} = [\,\kappa_y\,,\,\kappa_z\,]$ determines the direction of the *line of curvature*. Hence, the neutral axis is perpendicular to the line of curvature and intersects the y and z axis at $\bar{y}_n$ and $\bar{z}_n$, respectively. Along the neutral axis $\varepsilon = 0$, and the direction of the curvature vector $\boldsymbol{\kappa}$ defines the region of the cross-section with positive strain, as shown in Fig. 10.40. The direction of the curvature vector is determined by for instance the angle relative to the y-axis, which is given by the tangent relation

$$\tan\theta_\kappa = \frac{\kappa_z}{\kappa_y}\,. \tag{10.84}$$

The neutral axis is not only used to identify the regions of tension and compression. In fact the neutral axis and the line of curvature constitute a local basis, in which the strain distribution is described particularly simple. This is demonstrated in the following.

Strain distribution

The neutral axis represents the line with vanishing axial strain, i.e. $\varepsilon = 0$. Because of the linear strain distribution the strain increases linearly in the direction perpendicular to the neutral axis along the line of maximum curvature. Thus, along lines perpendicular to the neutral axis the strain varies linearly and along lines parallel to the neutral axis the strain is constant. This implies that the strain distribution is fully determined by a single linear variation along the line of curvature, as illustrated in Fig. 10.41. In the expression for the axial strain (10.27) the slope of the linear strain distribution is given by the curvatures κ_y and κ_z, which are the components of the curvature vector $\boldsymbol{\kappa}$. The slope of the resulting strain distribution along the line of curvature corresponds to the length of the curvature vector, which is

$$\kappa = |\boldsymbol{\kappa}| = \sqrt{\kappa_y^2 + \kappa_z^2}\,. \tag{10.85}$$

The curvature vector is fully determined by the direction given in (10.84) and the length given above in (10.85).

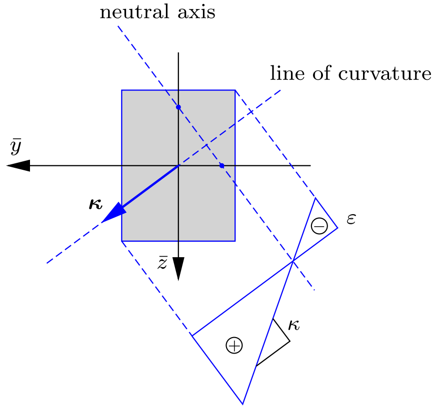

Fig. 10.41: Strain distribution with respect to neutral axis and line of curvature.

Example 10.16. Strain distribution for angle profile. Figure 10.42 shows the cantilever from Example 10.12, with tip loads P and $\frac{1}{2}P$ in the y and z direction, respectively. The moments at the fixed support are

$$M_y = -P\ell\,, \qquad M_z = -\tfrac{1}{2}P\ell\,,$$

and the inverse of the bending stiffness matrix has been found in Example 10.12:

$$\begin{bmatrix} I_{yy} & I_{yz} \\ I_{yz} & I_{zz} \end{bmatrix}^{-1} = \frac{3}{16} \begin{bmatrix} 5 & -6 \\ -6 & 20 \end{bmatrix} \frac{1}{a^3 t}.$$

The origin of the coordinate system $\{y, z\}$ is located at the elastic center C, determined in Example 10.1.

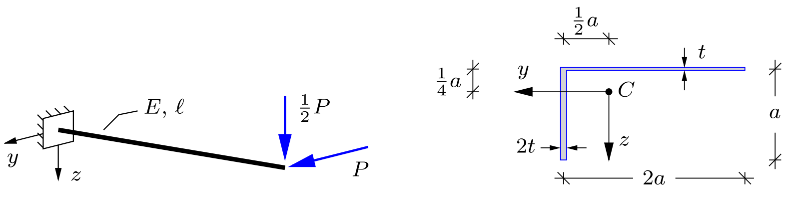

Fig. 10.42: Cantilever with angle profile and tip loads P and $\frac{1}{2}P$.

There is no axial loading of the beam, and thus

$$\varepsilon_c = \frac{1}{E_0} \frac{N}{F} = 0.$$

The neutral axis therefore passes through the elastic center and thereby the origin of the coordinate system. The direction of the neutral axis is determined via the curvature vector,

$$\begin{bmatrix} \kappa_y \\ \kappa_z \end{bmatrix} = \begin{bmatrix} I_{yy} & I_{yz} \\ I_{yz} & I_{zz} \end{bmatrix}^{-1} \begin{bmatrix} M_y \\ M_z \end{bmatrix} = -\frac{3}{16} \begin{bmatrix} 5 & -6 \\ -6 & 20 \end{bmatrix} \begin{bmatrix} 1 \\ \frac{1}{2} \end{bmatrix} \frac{P\ell}{E_0 a^3 t} = -\frac{3}{8} \begin{bmatrix} 1 \\ 2 \end{bmatrix} \frac{P\ell}{E_0 a^3 t}.$$

The angle of the curvature vector relative to the y-axis is found by (10.84),

$$\tan\theta_\kappa = \frac{\kappa_z}{\kappa_y} = 2 \qquad \Rightarrow \qquad \theta_\kappa = 63.4^\circ.$$

The curvature vector and the line of maximum curvature are shown in Fig. 10.43, and the neutral axis is shown as the line perpendicular to the line of maximum curvature. Both κ_y and κ_z are negative, and thus the curvature vector points into the fully negative quadrant of the coordinate system. This again implies that the region with tension (positive axial strain) is above the neutral axis, while the compression zone is below. The slope of the strain variation is obtained as the length of the curvature vector (10.85),

$$\kappa = \frac{3}{8}\sqrt{1^2 + 2^2}\, \frac{P\ell}{E_0 a^3 t} = \frac{3\sqrt{5}}{8} \frac{P\ell}{E_0 a^3 t} = 0.84 \frac{P\ell}{E_0 a^3 t}.$$

It is seen in Fig. 10.43 that the neutral axis intersects the corner of the cross-section in B, indicating that the axial strain is zero at this point. This agrees with the results obtained in Example 10.12, and shown in Table 10.1. The strain increases linearly in the direction of the line of curvature, and it is seen directly that the largest positive strain (tension) occurs in point C, while the largest negative strain (compression) occurs at the other free end in point A. The distance from the neutral axis to the point C is denoted as d in Fig. 10.43 and determined via the angle of the line of curvature:

$$\cos\theta_\kappa = \frac{d}{2a} \qquad \Rightarrow \qquad d = 2a\cos\theta_\kappa = \tfrac{2}{\sqrt{5}}\, a.$$

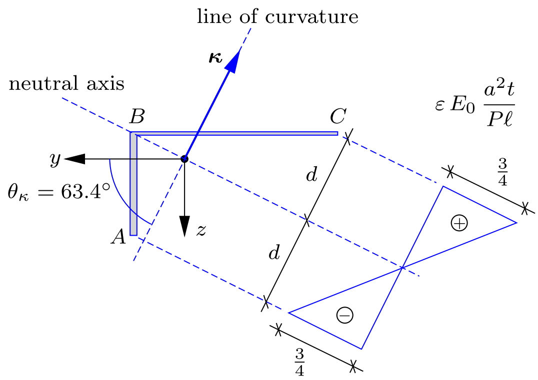

Fig. 10.43: Normalized strain distribution along line of curvature.

The strain at C is found as the distance d times the slope of the linear strain distribution κ:

$$\varepsilon_C = \kappa\, d = \frac{3\sqrt{5}}{8}\,\frac{P\ell}{E_0 a^3 t}\,\frac{2}{\sqrt{5}}\,a = \frac{3}{4}\,\frac{P\ell}{E_0 a^2 t}\,,$$

corresponding to the result obtained in Example 10.12. It turns out that the distance from the neutral axis to point A is also d, whereby $\varepsilon_A = -\varepsilon_C$. □

Example 10.17. Strain distribution for Z-profile. Consider the simply supported beam in Fig. 10.44 with a Z-profile as cross-section. The strain and stress distribution has been determined in Example 10.13, and the present example determines the strain distribution with respect to the neutral axis and the line of curvature. The loading of the beam implies that the bending moments at the center section are

$$M_y^C = 0\,, \qquad M_z^C = \tfrac{1}{8}p\ell^2\,.$$

The normal force is zero. The coordinate system $\{y,z\}$ has its origin at the elastic center.

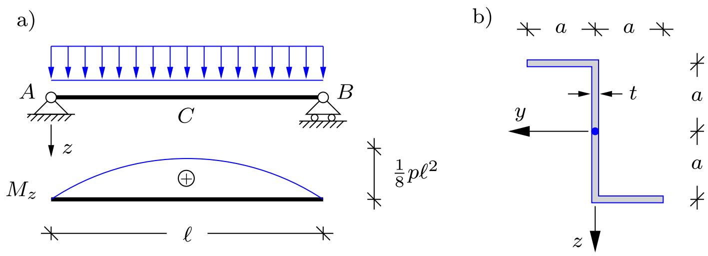

Fig. 10.44: Simply supported with with distributed load.

The moments of inertia with respect to the coordinate system, shown in Fig. 10.44b, have been determined in Example 10.13, and the curvature vector can therefore been found as

$$\begin{bmatrix}\kappa_y\\ \kappa_z\end{bmatrix} = \begin{bmatrix}I_{yy} & I_{yz}\\ I_{yz} & I_{zz}\end{bmatrix}^{-1}\begin{bmatrix}M_y^C\\ M_z^C\end{bmatrix} = \frac{3}{56}\begin{bmatrix}8 & 3\\ 3 & 2\end{bmatrix}\begin{bmatrix}0\\ 1\end{bmatrix}\frac{p\ell^2}{E_0 a^3 t} = \frac{3}{56}\begin{bmatrix}3\\ 2\end{bmatrix}\frac{p\ell^2}{E_0 a^3 t}\,.$$

The direction of the curvature vector is defined by the tangent relation

$$\tan\theta_\kappa = \frac{\kappa_z}{\kappa_y} = \tfrac{2}{3} \qquad \Rightarrow \qquad \theta_\kappa = 33.7^\circ\,.$$

The curvature vector $\boldsymbol{\kappa}$ and the associated line of curvature are shown in Fig. 10.45. Because the components of the curvature vector are positive it is located in the positive $\{y, z\}$ quadrant. The associated neutral axis is perpendicular to the line of curvature, and because $N = 0$ it contains the elastic center.

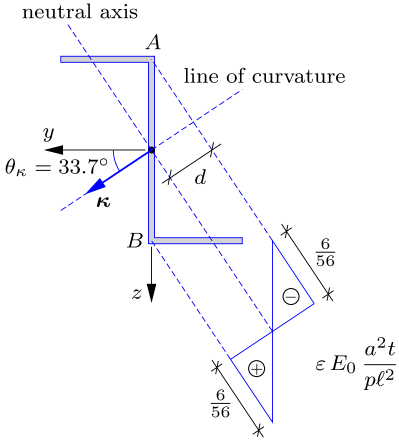

Fig. 10.45: Normalized strain distribution along line of curvature.

The linear strain variation along the line of maximum curvature is now determined. The slope of the linear variation is determined as the length of the curvature vector:

$$\kappa = \frac{3}{56}\sqrt{3^2+2^2}\,\frac{p\ell^2}{E_0a^3t} = \frac{3\sqrt{13}}{56}\,\frac{p\ell^2}{E_0a^3t} = 0.193\,\frac{p\ell^2}{E_0a^3t}\,.$$

The axial strain variation along the line of curvature is hereby determined as the slope κ times the distance from the neutral axis. Consequently, the largest strains occur at the points on the cross-section with greatest distance d to the neutral axis, which are the corners A and B, as shown in Fig. 10.45. The distance d is determined by the geometric relation:

$$\sin\theta_\kappa = \frac{d}{a} \qquad \Rightarrow \qquad d = a\,\sin\theta_\kappa = \tfrac{2}{\sqrt{13}}\,a\,,$$

whereby the strains at corners A and B are:

$$\varepsilon_A = -\,\kappa\,d = -\,\frac{6}{56}\,\frac{p\ell^2}{E_0a^2t}\,, \qquad \varepsilon_B = \kappa\,d = \frac{6}{56}\,\frac{p\ell^2}{E_0a^2t}\,.$$

The sign of the axial strain follows from the direction of the curvature vector, see Fig. 10.45. The above values for the strain in A and B correspond to the results obtained in Example 10.13, see Fig. 10.35b. □

10.4 Exercises

Exercise 10.1. The figure shows the angle profile considered in Example 10.1. In this exercise the reference coordinate system is shown in the figure with origin at the right end of the horizontal flange. Assume that the cross-section is homogeneous with $E_1 = E_2 = E_0$, and $t_1 = t_2 = t$, $a_1 = 2a$ and $a_2 = a$. The cross-section can be considered as thin-walled with $t \ll a$.

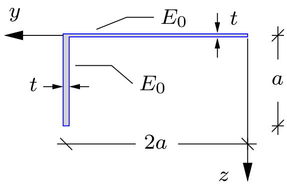

a) Determine the static moments S_y and S_z with respect to the reference axes.

b) Determine the location of the elastic center and compare with the results of Example 10.1.

Exercise 10.2. The figure shows the T-profile considered in Example 10.2. In this exercise the reference coordinate system is shown in the figure with origin at the right end of the horizontal flange. Assume that the cross-section is homogeneous with $E_f = E_w = E_0$, and $a_f = a_w = a$, $t_w = t$ and $t_f = 3t$. The cross-section can be considered as thin-walled with $t \ll a$.

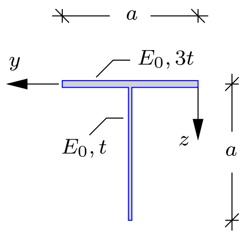

a) Determine the static moments S_y and S_z with respect to the reference axes.

b) Determine the location of the elastic center and compare with the results of Example 10.2.

c) Locate the coordinate system $\{\bar{y}, \bar{z}\}$ with origin in the elastic center, and determine the moments of inertia $I_{\bar{y}\bar{y}}$, $I_{\bar{z}\bar{z}}$ and $I_{\bar{y}\bar{z}}$.

Exercise 10.3. The figure shows a homogeneous C-profile with elastic modulus $E = E_0$. The height of the cross-section is h and the width is b. The thickness of the web is t, while the flange thickness is $2t$. The cross-section can be considered as thin-walled with $t \ll h, b$.

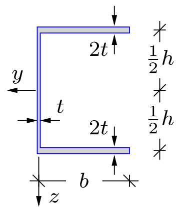

a) Choose the coordinate system $\{y, z\}$ shown in the figure and determine the location of the elastic center $[c_y, c_z]$.

b) Locate the coordinate system $\{\bar{y}, \bar{z}\}$ with origin in the elastic center, and determine the moments of inertia $I_{\bar{y}\bar{y}}$, $I_{\bar{z}\bar{z}}$ and $I_{\bar{y}\bar{z}}$ when $h = b = a$.

Exercise 10.4. The figure shows a homogeneous C-profile with elastic modulus $E = E_0$. The height of the cross-section is $3a$, the width is $2a$ and the thickness is t, as shown in the figure. The cross-section can be considered as thin-walled with $t \ll a$.

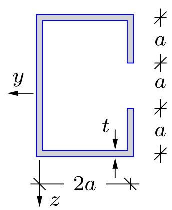

a) Choose a suitable coordinate system $\{y, z\}$ and determine the location of the elastic center $[c_y, c_z]$.

b) Locate the coordinate system $\{\bar{y}, \bar{z}\}$ with origin in the elastic center, and determine the moments of inertia $I_{\bar{y}\bar{y}}$, $I_{\bar{z}\bar{z}}$ and $I_{\bar{y}\bar{z}}$.

c) Consider the section forces: $N = 0$ and $M_{\bar{y}} = M_{\bar{z}} = \bar{M}$, and determine the axial strain distribution ε.

d) Determine the maximum axial stress $\sigma_{\max}$.

Exercise 10.5. The figure shows an inhomogeneous I-profile cross-section. The top flange has dimensions $2a \times t$ and elastic modulus E_f. The web has dimensions $2a \times \frac{1}{5}t$ and elastic modulus $10E_f$. And finally, the bottom flange has dimensions $a \times \frac{1}{5}t$ and elastic modulus $10E_f$. The cross-section can be considered as thin-walled with $t \ll a$.

a) Choose a suitable coordinate system $\{y, z\}$ and determine the location of the elastic center $[c_y, c_z]$.

b) Locate the coordinate system $(\bar{y}, \bar{z})$ with origin in the elastic center, and determine the moments of inertia $I_{\bar{y}\bar{y}}$, $I_{\bar{z}\bar{z}}$ and $I_{\bar{y}\bar{z}}$.

c) Assume the section forces: $N = 0$, $M_{\bar{y}} = 0$ and $M_{\bar{z}} = \bar{M}$, and determine the axial strain distribution ε.

d) Find the axial stress in the top flange and in the bottom flange, respectively.

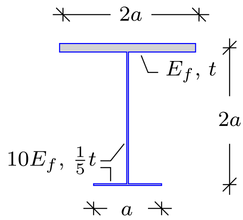

Exercise 10.6. The figure shows the rectangular cross-section made of concrete with steel reinforcement. The elastic modulus of concrete is E_c, and the elastic modulus of the steel reinforcement is $E_s = 15E_c$. The total area of reinforcement is $A_s = a^2/50$. The location of the elastic center has been determine in Example 10.3.

a) Locate the coordinate system $\{\bar{y}, \bar{z}\}$ with origin in the elastic center, and determine the moments of inertia $I_{\bar{y}\bar{y}}$, $I_{\bar{z}\bar{z}}$ and $I_{\bar{y}\bar{z}}$.

b) Consider the section forces: $N = 0$, $M_{\bar{y}} = 0$ and $M_{\bar{z}} = \bar{M}$, and determine the axial strain distribution ε.

c) Determine both the maximum tension and compression stress in the concrete, and the maximum stress in the steel reinforcement.

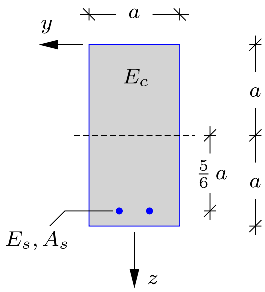

Exercise 10.7. Consider the T-profile in Example 10.7, that is shown in the figure below. The moments of inertia with respect to the axes with origin at the elastic center is given in Example 10.7. In the following the normal force $N = 0$.

a) Determine the distribution of axial strain ε and the maximum axial stress $\sigma_{\max}$ for the loading $M_y = \bar{M}$ and $M_z = 0$.

b) Repeat a) for $M_y = 0$ and $M_z = -2\bar{M}$.

c) Use the results in a) and b) to determine the distribution of axial strain ε and the maximum axial stress $\sigma_{\max}$ for the combined load case $M_y = \bar{M}$ and $M_z = -2\bar{M}$.

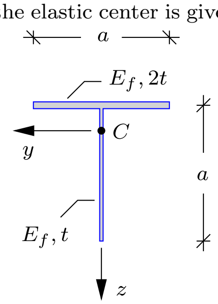

Exercise 10.8. Consider the Z-profile in Example 10.10. Draw Mohr's circle and determine the principal moments of inertia $I_{y'}$ and $I_{z'}$ graphically. Compare with the result obtained in the example.

Exercise 10.9. The figure shows a Z-profile with height $2a$ and width a, and thickness t. The cross-section is homogeneous with elastic modulus $E = E_0$. It is loaded by bending moments $M_y = \bar{M}$ and $M_z = 2\bar{M}$. The cross-section can be considered as thin-walled with $t \ll a$.

a) Determine the moments of inertia I_{yy}, I_{zz} and I_{yz}.
b) Determine the principal moments of inertia $I_{y'}$ and $I_{z'}$, and the orientation of the principal axes.
c) Draw Mohr's circle.
d) Determine the curvatures κ_y and κ_z, and draw the line of curvature and the neutral axis.
e) Determine the distribution of the axial strain ε and find the maximum axial stress $\sigma_{\max}$.

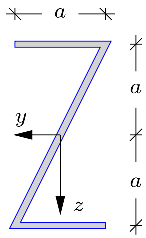

Exercise 10.10. The figure shows a Z-profile similar to that in the previous exercise, but with additional vertical flanges. The geometry is shown in the figure below and the thickness is t. The cross-section is homogeneous with elastic modulus $E = E_0$. It is loaded by bending moments $M_y = \bar{M}$ and $M_z = 2\bar{M}$. The cross-section can be considered as thin-walled with $t_f \ll a$.

a) Determine the moments of inertia I_{yy}, I_{zz} and I_{yz}.
b) Determine the principal moments of inertia $I_{y'}$ and $I_{z'}$, and the orientation of the principal axes.
c) Draw Mohr's circle.
d) Determine the curvatures κ_y and κ_z, and draw the line of curvature and the neutral axis.
e) Determine the distribution of the axial strain ε and find the maximum axial stress $\sigma_{\max}$.